Parasitology Research (2021) 120:2595–2616
https://doi.org/10.1007/s00436-021-07152-5

PROTOZOOLOGY - ORIGINAL PAPER

A discovery of two new *Tetrahymena* species parasitizing slugs and mussels: morphology and multi-gene phylogeny of *T. foissneri* sp. n. and *T. unionis* sp. n.

Tengyue Zhang[1] · Peter Vďačný[1]

Received: 16 February 2021 / Accepted: 4 April 2021 / Published online: 14 April 2021

Abstract

The presence of parasitic ciliates of the hymenostome genus *Tetrahymena* was examined in 150 mollusks belonging to six bivalve and 13 gastropod species in Slovakia, Central Europe. Tetrahymenids were detected only in two species, viz., in the invasive Lusitanian slug (*Arion vulgaris*) and in the native swollen river mussel (*Unio tumidus*). Although only 10.52% of the examined mollusk taxa were positive, their *Tetrahymena* infections were very intensive accounting for several hundreds of ciliates per host. Phylogenetic analyses of the 16S and 18S rRNA genes as well as of the barcoding region of the gene encoding for cytochrome *c* oxidase subunit I revealed that both isolates represent new taxa, *T. foissneri* sp. n. and *T. unionis* sp. n. The former species belongs to the '*borealis*' clade and its nearest relative is *T. limacis*, a well-known parasite of slugs and snails. Besides molecular data, *T. foissneri* can be distinguished from *T. limacis* also morphologically by the body shape of the parasitic-phase form, dimensions of micronuclei, and the silverline system. On the other hand, *T. unionis* was classified within the '*paravorax*' clade along with *T. pennsylvaniensis*, *T. glochidiophila*, and *T. nigricans*. Although these four species are genetically distinct, *T. unionis* could be morphologically separated only from *T. nigricans* by body shape and size. The present study suggests that both aquatic and terrestrial mollusks represent interesting hosts for the discovery of novel *Tetrahymena* lineages.

Keywords *Arion vulgaris* · Ciliophora · Hymenostomatia · Histophagy · Mollusca · *Unio tumidus*

Introduction

The genus *Tetrahymena* Furgason, 1940 comprises not only free-living representatives, which occur in a variety of freshwater and soil habitats (e.g., Corliss 1973; Doerder 2014, 2019; Foissner 1987, 1998, 2000; Pitsch et al. 2017; Quintela-Alonso et al. 2013; Zahid et al. 2014), but also endoparasites or commensals, which inhabit a variety of animals including planarians, mollusks, insects, fish, and even mammals (e.g., Corliss 1960; Lynn et al. 2000, 2018; Rataj and Vďačný 2020; Van As and Basson 2004). The common morphological feature of this genus is the oral apparatus that is composed of four ciliary structures, i.e., a paroral membrane and three oral polykinetids (Furgason 1940). Corliss (1969, 1970) provided the first insights into the intrageneric taxonomy of *Tetrahymena* and recognized three groups: (1) the *pyriformis* complex, containing bacteria-feeding microphagous ciliates with tendencies to become parasites; (2) the *rostrata* complex, gathering facultative histophagous and/or parasitic species often dividing inside of a cyst; and (3) the *patula* complex of non-parasitic, weakly histophagous but occasionally cannibalistic macrostome forms. However, Corliss' three complexes were useful constructs at the time, and they have long since been abandoned as they have no phylogenetic relevance. Moreover, distinguishing species within the three complexes based solely on morphological characteristics was very difficult because most *Tetrahymena* species share a rather similar body shape and size as well as a uniform somatic ciliature and overlapping numbers of ciliary rows. Therefore, DNA barcoding based especially on the mitochondrial gene encoding for cytochrome *c* oxidase subunit 1 (COI) was employed to identify morphologically highly similar species that also might possess identical 18S rRNA gene sequences (e.g., Doerder 2019; Lynn and Strüder-Kypke

Handling Editor: Julia Walochnik

✉ Peter Vďačný
peter.vdacny@uniba.sk

[1] Department of Zoology, Faculty of Natural Sciences, Comenius University in Bratislava, 842 15 Bratislava, Slovakia

2006; Rataj and Vďačný 2020; Simon et al. 2008). Molecular taxonomic methods became a standard and a quite unambiguous method for separation of *Tetrahymena* species, as the intraspecific variation is typically up to 2% while the interspecific variation ranges from about 4 to 11% in the COI gene (Chantangsi et al. 2007; Doerder 2014, 2019; Kher et al. 2011; Lynn and Doerder 2012; Rataj and Vďačný 2020). Despite the intensive research in the past decades, it is still hard to determine the overall species richness within the genus *Tetrahymena*, as many habitats and potential host organisms remain to be studied.

Although *Tetrahymena* infections have been comparatively rarely recorded, there are distinctly more reports from aquatic than from terrestrial animals. More specifically, tetrahymenid endoparasites were already found in freshwater planarians (Rataj and Vďačný 2020; Reynoldson and Bellamy 1973; Wright 1969, 1981), in black flies, alderflies, mosquitoes, and midges (Batson 1983, 1985; Corliss 1960; Jerome et al. 1996; Lynn et al. 1981), in larvae of freshwater bivalves (Lynn et al. 2018; Prosser et al. 2018), in adult crayfish (Edgerton et al. 1996), and in a broad variety of fish ranging from guppies (e.g., Hatai et al. 2001; Hoffman et al. 1975; Imai et al. 2000) to salmons (Ferguson et al. 1987). In contrast, there is just a single report of *Tetrahymena* parasitizing terrestrial vertebrates, namely *T. farleyi* Lynn et al., 2000, which was isolated from the urine of a Dalmatian dog (Lynn et al. 2000). As concerns terrestrial invertebrates, *Tetrahymena* infections have been mostly reported from various slugs and snails (for a review, see Van As and Basson 2004). Nevertheless, mollusks still represent an insufficiently explored host-group of *Tetrahymena* species (Antipa and Small 1971; Corliss 1960; Prosser et al. 2018; Van As and Basson 2004). In the present contribution, we examined 150 specimens belonging to 19 bivalve and gastropod species. *Tetrahymena* species were, however, detected only twice. Analyses of their 16S and 18S rRNA genes as well as of their COI gene demonstrated significant genetic differences, justifying the establishment of two new species, *T. foissneri* sp. n. and *T. unionis* sp. n.

Material and methods

Material collection and processing

Altogether, 105 terrestrial mollusks belonging to 11 species were collected at 10 localities, and 45 aquatic mollusks belonging to eight species were sampled at five localities in Slovakia, Central Europe (Supplementary Table S1). Tetrahymenid ciliates were detected only in two species, viz., in the invasive Lusitanian slug, *Arion vulgaris* (Moquin-Tandon, 1855), collected from a sidewalk at the Stratená ulica street, Bratislava (48° 12′ 11″ N, 17° 09′ 04″ E) on November 11, 2019, and in the swollen river mussel, *Unio tumidus* (Philipsson, 1788), collected from the River Hornád near the village of Milhosť, south of the city of Košice (48° 31′ 45″ N, 21° 18′ 20″ E) on May 10, 2020. Sampled mollusks were transferred together with in situ substrates to the laboratory at the Department of Zoology, Comenius University in Bratislava. Slugs were directly dissected; their digestive (esophagus, stomach, digestive gland, and gut), reproductive (albumen gland, ovotestis), and excretory (kidney) organs were extracted and investigated for the presence of ciliates. The mantle cavity of mussels was rinsed with water using a micropipette before dissection. Ciliates were found in great abundance in water expelled from the mantle cavity and the excurrent siphon of mussels when they were placed in Petri dishes containing tap water. The extruded water contained much organic debris and peeled off epithelial tissues as well. After rinsing the mantle cavity, mussels were dissected, and their internal organs were examined for the presence of ciliates. Tetrahymenid ciliates were manually picked with the aid of Pasteur micropipettes adjusted as described by Foissner (2014). Cultures of both isolated *Tetrahymena* species were established in Petri dishes, using tap water as a medium and pieces of host tissues as a food source. Cultures were maintained for several months in a refrigerator at a temperature of 6 °C. This temperature was chosen, as both species were sampled during cooler parts of the year. No attempts to establish axenic cultures were made, as both *Tetrahymena* species thrived on host tissues.

Taxonomic and molecular methods

Living ciliates were investigated under an optical microscope Zeiss Axio Imager 2 (Carl Zeiss, Oberkochen, Germany) equipped with differential interference contrast optics at low and high magnifications. The ciliary and silverline pattern and the nuclear apparatus were revealed with the dry silver nitrate (Klein 1958) and protargol (Wilbert 1975) impregnation methods. Only fresh material was used for living observations and all staining procedures, as some morphological features might change during cultivation. Microphotographs were captured by a Canon EOS 80D camera (Canon Inc., Ota City, Tokyo, Japan). In vivo measurements were based on microphotographs and were carried out with the help of the calibrated software ImageJ ver. 1.49 (Schneider et al. 2012). Measurements on mounted specimens were conducted with an ocular micrometer. Illustrations were prepared in Inkscape ver. 0.92.4 and Adobe Photoshop CC. Terminology mostly follows Lynn (2008).

Individual cells of both tetrahymenid species were put in 180 μl of cell lysis buffer (Promega, Fitchburg, WI, USA) and stored at 6 °C pending DNA extraction. Five single-cell samples were prepared for *T. foissneri* sp. n. and four single-cell samples for *T. unionis* sp. n. The extraction of genomic DNA,

PCR amplification, and sequencing followed our previous study on tetrahymenids parasitizing planarians (Rataj and Vďačný 2020). PCR primers are summarized in Table 1 and PCR conditions are listed in Table 2. Electropherograms of the newly obtained sequences were carefully inspected in Chromas ver. 2.6.6 (Technelysium Pty Ltd., South Brisbane, Australia), trimmed and assembled into contigs using BioEdit ver. 7.2.5 (Hall 1999).

Type and localization of unique nucleotides suitable for taxa diagnoses were searched for in the barcoding region of the COI gene, using a custom Python script. The query group contained all specimens of the species in question, while the reference group comprised their nearest relatives, as revealed by the BLASTn search and the present phylogenetic analyses. The reference alignments are provided in Supplementary material (Alignments 1 and 2). Only nucleotide states that were shared by all members of the query group and were different from the states in the reference group were used as diagnostic characters.

The ZooBank registration number of the present work is urn:lsid:zoobank.org:pub:41559C77-2CB2-4AA3-BD58-05C9974CD5B3.

Phylogenetic methods

To determine the phylogenetic positions of the two new *Tetrahymena* species, four datasets were assembled. The first dataset contained 108 concatenated sequences of the nuclear 18S rRNA gene and the mitochondrial COI gene (for taxon sampling and GenBank accession numbers, see Supplementary Table S2). The second alignment contained 114 COI sequences, and the third alignment consisted of 95 sequences coding for the 16S rRNA molecule (GenBank entries are shown in respective figures). The fourth dataset consisted of 30 concatenated sequences of two mitochondrial markers, the 16S rRNA and the COI gene (Supplementary Table S3). Taxon sampling in all datasets followed Doerder (2019) and Rataj and Vďačný (2020).

16S and 18S rRNA gene sequences were aligned using the MAFFT algorithm on the GUIDANCE2 server (http://guidance.tau.ac.il/ver2/) (Sela et al. 2015), with parameters as specified in Zhang and Vďačný (2020). The protein-coding COI gene sequences were aligned, using amino acid sequences as predicted with the invertebrate mitochondrial genetic code in MEGA X ver. 10.2 (Kumar et al. 2018). The COI alignment was divided into three partitions, each representing one codon position, using a custom Python script. Three different algorithms were used to build phylogenetic trees: neighbor-joining (NJ) as implemented in MEGA X (Kumar et al. 2018), maximum likelihood (ML) as implemented in IQ-Tree ver. 1.6.10 (Nguyen et al. 2015), and Bayesian inference as implemented in MrBayes ver. 3.2.7 (Ronquist et al. 2012). NJ analyses included the maximum composite likelihood method, gamma-distributed rates among sites, a heterogeneous pattern among lineages, a pairwise deletion option to exclude alignment gaps, and 5000 bootstrap replicates. ML analyses had the following settings: a starting BioNJ tree; each partition was allowed to have a different speed; the best fitting evolutionary substitution models were selected for each partition under the BIC criterion using the in-built ModelFinder program; 1000 ultrafast bootstrap replicates; and the bnni algorithm to reduce overestimating nodal support (Hoang et al. 2018). Bayesian inference included Markov chain Monte Carlo (MCMC) simulations, which were run for three to ten million generations with a sampling frequency of 100. Two different programs, jModelTest ver. 2.1.10 (Darriba et al. 2012) and IQ-Tree (Nguyen et al. 2015), were used to determine the best evolutionary model and its parameters for each molecular marker/codon partition. Parameters of the evolutionary models used are listed in Supplementary Table S4 and S5. Convergence of MCMC analyses was inspected using the in-built diagnostics of MrBayes. Results of convergence analyses are summarized in Supplementary Table S6. Given the results of these analyses, we present here Bayesian trees inferred from the first, third, and fourth datasets under the IQ-Tree evolutionary models and a Bayesian tree inferred from the second dataset under the jModelTest evolutionary models. The first 25% of sampled trees were considered as the burn-in fraction, and they were excluded before the construction of 50%-majority rule consensus trees. ML and Bayesian analyses were conducted on the CIPRES portal ver. 3.1 (http://www.phylo.

Table 1 Primers used for amplification of three molecular markers analyzed in two new *Tetrahymena* species parasitizing slugs and mussels

Molecular marker	Primer name	Primer sequence (in 5' to 3' direction)	Reference
18S rRNA gene	Euk A	AAC CTG GTT GAT CCT GCC AGT	Medlin et al. (1988)
	Euk B	TGA TCC TTC TGC AGG TTC AC	Medlin et al. (1988)
16S rRNA gene	16S-mtSSU-F	TGT GCC AGC AGC CGC GGT AA	van Hoek et al. (2000)
	16S-mtSSU-R	CCC MTA CCR GTA CCT TGT GT	van Hoek et al. (2000)
Cytochrome *c* oxidase subunit I	COI-FW-mod	ATG TGA GTT GAT TTT ATA GA	Chantangsi et al. (2007)
	COI-689-RW	CTC TTC TAT GTC TTA AAC CAG GCA	Doerder (2014)

Table 2 Conditions of PCR reactions used for amplification of three molecular markers analyzed in two new *Tetrahymena* species parasitizing slugs and mussels

Molecular marker	PCR program (number of cycles, temperature/time)								Reference
	Stage I	Stage II			Stage III			Stage IV	
18S rRNA gene	1×	–			30×			1×	Vďačný et al. (2011)
	95 °C/15 min	–	–	–	95 °C/45 s	55 °C/60 s	72 °C/150 s	72 °C/10 min	
16S rRNA gene	1×	5×			30×			1×	Lynn and Strüder-Kypke (2006)
	94 °C/3 min	94 °C/30 s	50 °C/60 s	68 °C/75 s	94 °C/30 s	60 °C/60 s	68 °C/75 s	68 °C/10 min	
Cytochrome *c* oxidase subunit I	1×	5×			35×			1×	Rataj and Vďačný (2020)
	94 °C/3 min	94 °C/30 s	45°C/60 s	68 °C/75 s	94 °C/30 s	55 °C/60 s	68 °C/75 s	68 °C/10 min	

org/) (Miller et al. 2010). All trees were computed as unrooted and were rooted using the outgroup taxa in FigTree ver. 1.2.3 (http://tree.bio.ed.ac.uk/software/ figtree/).

Bayesian delimitation of four closely related *Tetrahymena* species within the '*paravorax*' clade (*T. glochidiophila*, *T. pennsylvaniensis*, *T. nigricans*, and *T. unionis*) was performed with the program BP&P ver. 2.2 (Yang 2015). The coalescent analyses were based on two markers, the nuclear 18S rRNA gene and the mitochondrial COI gene. Species delimitation together with estimation of a species tree was conducted using the following settings: a gamma prior for the θ parameter at $G(1, 660)$ and a gamma prior for the τ parameter at $G(14, 520)$; divergence times and rates among individual markers as estimated from the Dirichlet distribution (Yang and Rannala 2010); heredity scalars of individual markers as estimated from the data using a gamma prior $G(4, 4)$; and a large fine-tuning parameter ($\varepsilon = 15$) assigned to the reversible jump (rj) algorithm to guarantee a good mixing. The θ and τ parameters were estimated by running an A00 analysis. The posterior distribution and mean of both parameters at the root were calculated from the log file in Tracer ver. 1.7 (Rambaut et al. 2018). Consequently, the posterior distributions were fitted with a gamma distribution. During rjMCMC simulations, every second iteration was taken, the first 100,000 samples were discarded as burn-in, and one million samples were saved. The maximum clade credibility species tree was calculated in TreeAnnotator ver. 2.6.0 (Bouckaert et al. 2014).

Results

Description of *Tetrahymena foissneri* sp. n.

ZooBank registration number: urn:lsid:zoobank.org:act:8EE817FB-292F-440B-B79D-B6EB31E4783B.

Diagnosis: Size about 35–58 × 20–37 μm in vivo. Body narrowly ovoidal to ovoidal, anterior end acute, posterior end broadly rounded. Macronucleus globular to ellipsoidal, a single globular micronucleus. Contractile vacuole dorsal and subterminal, two or three excretory pores. About 25 to 34 ciliary rows including two or three postoral kineties. Oral apparatus about 9–11 μm long, forming a *Tetrahymena*-like pattern. Silverline system composed of primary meridians connecting kinetids and secondary meridians running in parallel and regularly alternating with primaries. No caudal cilia.

Diagnostic molecular characters in COI gene (with respect to *T. limacis* EF070288): 3 C, 9 C, 12 C, 16 C, 32 G, 54 T, 55 C, 78 G, 114 T, 141 C, 168 A, 195 T, 201 C, 237 G, 252 T, 297 C, 300 T, 309 C, 321 G, 324 T, 333 A, 345 C, 348 T, 351 T, 354 C, 384 A, 414 A, 426 G, 468 C, 471 C, 484 T, 510 T, 515 C, 516 T, 517 G, 557 T, 561 T, 582 G, 606 C, 612 C, 613

T, 615 T, 672 A, 703 A, 708 G, 726 T, 765 A, 783 A, 786 G, 800 C, 804 A, 819 T, 831 T, 843 G, 847 G, 885 T, 909 T.

Type locality: A sidewalk at Stratená ulica street, Bratislava, Slovakia (48° 12′ 11″ N, 17° 09′ 04″ E).

Type host: *Arion vulgaris* (Moquin-Tandon, 1855).

Type material: A DNA sample of holotype specimen has been deposited in Natural History Museum, Vajánskeho nábrežie 2, 810 06 Bratislava, Slovakia (ID Collection Code 01427572).

Additional material: One paratype slide containing protargol-impregnated specimens (reg. no. 2021/1-ZTY) and one paratype slide containing silver nitrate-impregnated specimens (reg. no. 2021/2-ZTY) have been deposited at Department of Zoology, Comenius University in Bratislava, Ilkovičova 6, 842 15 Bratislava, Slovakia.

Gene sequences: The nuclear 18S rRNA gene, the mitochondrial 16S rRNA gene, and the mitochondrial cytochrome *c* oxidase subunit I sequences of the holotype specimen have been deposited in GenBank (https://www.ncbi.nlm.nih.gov/genbank/) under the following accession nos. MW827176, MW827185, and MW828683, respectively.

Dedication: We named this species in memory of an outstanding protistologist, Prof. Dr. Wilhelm Foissner (1948–2020), Paris Lodron University of Salzburg, Salzburg, Austria, as a small token of appreciation for guiding many students into ciliatology, for altruistic sharing of his great knowledge, and for his constructive criticism, which made people think and work scientifically.

Description: Body size in vivo approximately 35–58 × 20–37 μm, with a length:width ratio of about 1.3–1.8:1 (n = 13). Shape narrowly ovate to ovate, anterior end acute, posterior end broadly rounded; flexible but not contractile (Figs. 1a, d–g; 2a–c; and 3i, j). Macronucleus typically located in body center, globular to ellipsoidal in vivo and after methyl green staining, sometimes slightly deformed and with irregular surface after protargol impregnation, on average 12.3 μm in largest diameter after protargol impregnation; nucleoli numerous, globular, and evenly distributed over macronuclear surface. Micronucleus nearby or attached to macronucleus, globular and about 2.2–3.5 μm in largest diameter after protargol impregnation (Figs. 1a, c–h; 2d–f; 3a, b, d–f; and Table 3). A single conjugation pair observed after methyl green staining, each partner contained a degenerating macronuclear nodule and two or three maturation derivatives (Fig. 2g). One contractile vacuole located dorsally and distinctly subterminally, about 4.5–6.5 μm across during diastole; two or three excretory pores well recognizable after protargol impregnation (Figs. 1a, d–h; 2a, c, e, f; and 3e, h). Cytoplasm colorless, studded with innumerable lipid droplets about 0.3–1.5 μm across and some food vacuoles about 3.5–5.5 μm across (Figs. 1a and 2c, d). Cortex flexible, no cortical granules recognizable. Locomotion by slowly swimming and rotating about longitudinal body axis or rarely by gliding on the bottom of Petri dish. Feeds on host tissues and possibly also on bacteria in cultures.

Somatic cilia about 5–8 μm long in vivo, slightly more densely spaced anteriorly than posteriorly, arranged in 25–34 meridional rows (Table 3). Two or three postoral ciliary rows, begin just behind oral apparatus and extend to rear body end. Ventral ciliary rows start from almost anterior body end to mid-portion of oral apparatus, run right and left of buccal cavity to reach posterior body pole. Lateral and dorsal ciliary rows commence subapically leaving an unciliated apical area, follow body curvature to terminate in posterior body region. All ciliary rows consist of monokinetids, except for lateral and dorsal kineties which begin with a dikinetid each. Anterior dikinetids form a paratene (circle) around unciliated apical area (Figs. 1a–c, h–j, l; 2d–f; and 3a, b, e, g, l–j). A more or less distinct suture made by ventral ciliary rows, extends from apical body end to beginning of oral apparatus (Figs. 1b and 3a, c). Caudal cilium not observed in vivo, no basal bodies recognizable in posterior pole area after protargol and dry silver nitrate impregnation.

Silverline system composed of primary meridians connecting kinetids within somatic kineties and secondary meridians running in parallel and regularly alternating with primaries (Figs. 1i–l and 3i–m). Inconspicuous outgrowths (peaks) emerge on left side of primary meridians between each two kinetids. Secondary meridians unevenly dotted by deeply impregnated pellicular pores resembling basal bodies. Cross-silverlines loosely and irregularly branch off from primary meridians to connect with secondary meridians, forming rectangular and comparatively large meshes which resemble a platyophryid pattern (Fig. 1k).

Oral apparatus situated in a shallow cavity of ventral body side, i.e., in anterior fifth to third of body length, about 6.7–7.7 μm long after dry silver nitrate impregnation. Oral ciliature composed of a paroral membrane and three membranelles (oral polykinetids) as usual in tetrahymenids. Paroral membrane J-shaped and composed of very narrowly spaced dikinetids. Membranelle M1 longest (3.7 μm long after protargol impregnation), composed of four rows of basal bodies, anterior row about half of length of the three remaining rows. Membranelle M2 similar in fine structure to M1 but slightly shorter (3.3 μm long after protargol impregnation). Membranelle M3 inconspicuous because only ca. 2.0 μm long after protargol impregnation, composed of three or four rows gradually shortened from left to right (Figs. 1b, i, j; 2c; 3a, c, f, l; and Table 3).

Prevalence and intensity: *T. foissneri* was detected only in a single specimen of the Lusitanian slug *A. vulgaris*, which was sampled at the type locality. Although no signs of pathological changes were observed, a mass *Tetrahymena* infection (several hundred ciliates) was detected in the slug's digestive tract. During the years 2019–2020, altogether, 24 *A. vulgaris* specimens, originated from three further localities in the surroundings of the type locality of *T. foissneri*, were examined for the

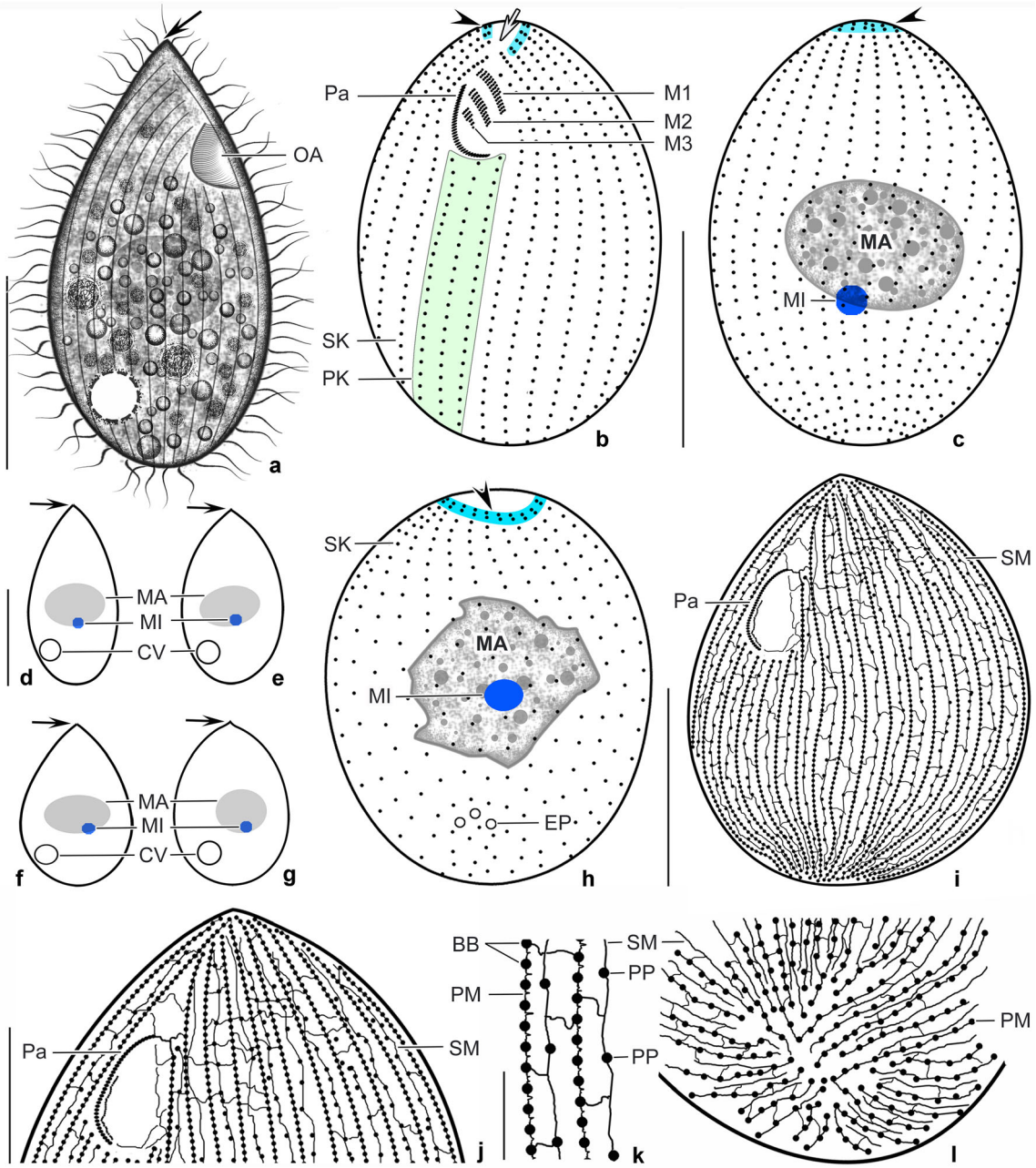

Fig. 1 *Tetrahymena foissneri* sp. n. from life (**a**, **d–g**), after protargol impregnation (**b**, **c**, **h**), and after dry silver nitrate impregnation (**i–l**). **a** Right view, showing the ovoid body. Black arrow indicates the acute anterior body end. **b, c** Ciliary pattern and nuclear apparatus of ventral and dorsal sides. Black arrowheads mark the anterior end of the ciliary rows which very likely begin with dikinetids (blue area) and white arrow shows the preoral suture. **d–g** Lateral overviews, showing the variability of body shape and size as well as of the nuclear apparatus, which consists of one macronuclear nodule (shaded grey) and a single micronucleus (shaded blue). Black arrows indicate the acute anterior body end. Drawn to scale. **h** Ciliary pattern of the right side. Black arrowhead marks the anterior dikinetids (blue area). **i** Ciliary and silverline pattern of the ventral side. **j–l** Details of the silverline system in the anterior (**j**) and posterior (**l**) body portions. The silverline system (**k**) consists of primary and secondary silverline meridians. *Explanations* = basal bodies (*BB*), contractile vacuole (*CV*), excretory pores (*EP*), macronucleus (*MA*), micronucleus (*MI*), oral apparatus (*OA*), paroral membrane (*Pa*), postoral kineties (*PK*), primary silverline meridian (*PM*), pellicular pores (*PP*), secondary silverline meridian (*SM*), somatic kineties (*SK*), adoral membranelles 1–3 (*M1–M3*). *Scale bars* = 2 μm (**k**), 8 μm (**j**, **l**), and 20 μm (**a–i**)

presence of ciliates (Supplementary Table S1). However, none was colonized by tetrahymenids. Likewise, any other investigated slug (*Deroceras* sp., *Limax maximus*, and *Tandonia kusceri*) or snail (*Alinda biplicata*, *Caucasotachea vindobonensis*, *Cepaea hortensis*, *Clausilia pumila*, *Cochlodina laminata*, *Helicodonta obvoluta*, *Helix pomatia*, and *Oxychilus* sp.) was infected by *Tetrahymena*, indicating that *T. foissneri* might be a rare species.

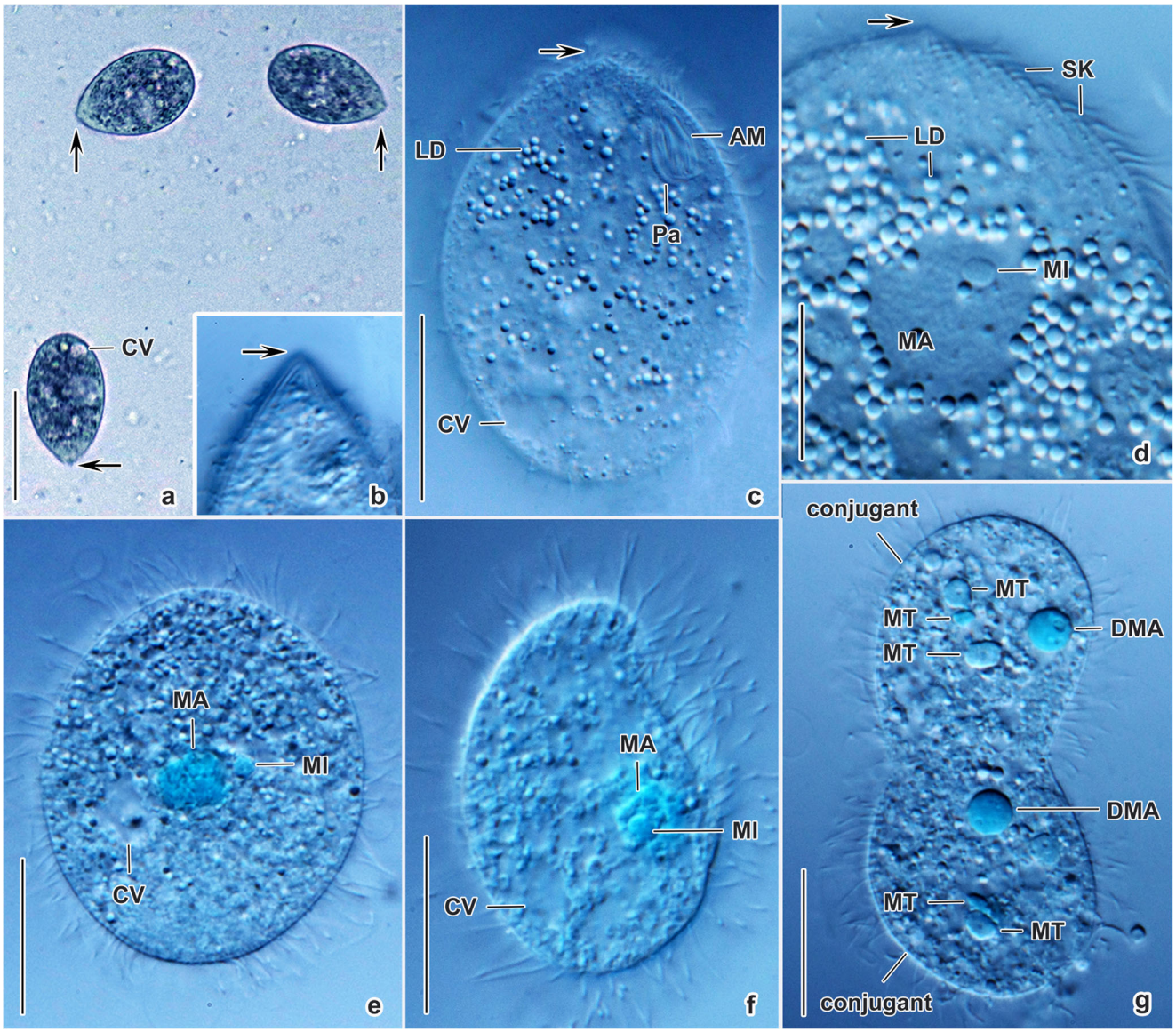

Fig. 2 *Tetrahymena foissneri* sp. n. from life (**a–d**) and after methyl green staining (**e–g**). **a** Overviews, showing some cells isolated from the gut of the slug *Arion vulgaris*. Arrows indicate the acute anterior body end. **b** Detail of the anterior body portion, showing the acute anterior body end (arrow). **c** Ventrolateral overview. Arrow indicates the narrowed anterior cell end. **d** Detail of the anterior body, showing the course of somatic kineties, the nuclear apparatus, and numerous lipid droplets. Arrow indicates the tapered anterior body end. **e–g** Overviews of the vegetative cells (**e, f**) and of a conjugation pair (**g**), showing the nuclear apparatus and contractile vacuoles. *Explanations* = adoral membranelles (*AM*), contractile vacuole (*CV*), degenerating macronuclear nodules (*DMA*), lipid droplets (*LD*), macronucleus (*MA*), micronucleus (*MI*), maturation derivatives (*MT*), paroral membrane (*Pa*), somatic kineties (*SK*). *Scale bars* = 12 μm (**d**), 20 μm (**c**, **e–g**), and 40 μm (**a**)

Description of *Tetrahymena unionis* sp. n.

ZooBank registration number: urn:lsid:zoobank.org:act:6399B30E-AC7D-4125-892F-2B587C329D57.

Diagnosis: Size about 35–65 × 18–40 μm in vivo. Body narrowly ellipsoidal to broadly ovoidal, anterior end slightly tapered, posterior end broadly to narrowly rounded. Macronucleus globular to ellipsoidal, a single globular micronucleus. Contractile vacuole dorsal and subterminal, two excretory pores. About 24 to 33 ciliary rows including two postoral kineties. Oral apparatus about 10–14 μm long, forming a *Tetrahymena*-like pattern. Silverline system composed of only primary meridians with relatively long outgrowths (peaks). One long caudal cilium.

Diagnostic molecular characters in COI gene (with respect to *T. glochidiophila* MF693881, *T. nigricans* MN991323, and *T. pennsylvaniensis* KJ028745): 60 G, 111 A, 123 G, 165 G, 184 C, 189 T, 195 C, 249 C, 270 C, 294 C, 303 C, 339 G, 345 A, 348 T, 354 A, 358 C, 363 C, 369 A, 426 G, 513 A, 531 T, 552 T, 669 C, 672 A, 681 C, 711 T, 747 A, 810 C, 822 G, 825 A.

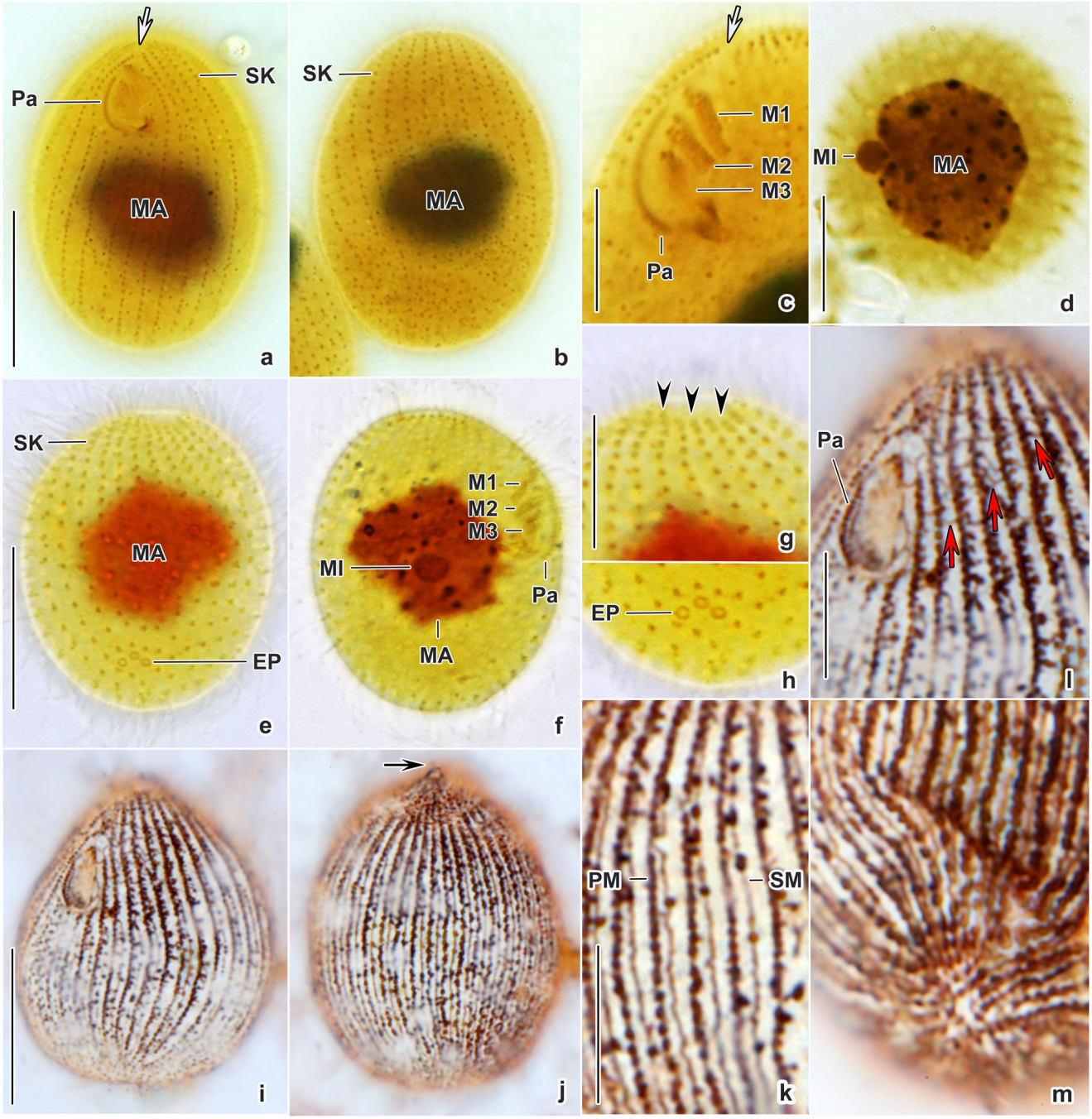

Fig. 3 *Tetrahymena foissneri* sp. n. after protargol (**a**–**h**) and after dry silver nitrate (**i**–**m**) impregnation. **a, b** Ciliary pattern and the nuclear apparatus of ventral (**a**) and dorsal (**b**) sides of a representative specimen. White arrow marks the preoral suture. **c** Detail of the oral apparatus, showing the paroral membrane and three adoral membranelles. White arrow marks the preoral suture. **d** Top view, showing the nuclear apparatus. **e**, **f** Right (**e**) and left (**f**) side overviews, showing the ciliary pattern and nuclear apparatus. **g**, **h** Detail of the anterior (**g**) and posterior (**h**) body portions. Black arrowheads mark the dikinetids at the anterior end of the ciliary rows. **i**, **j** Overviews, showing the silverline system on the ventral (**i**) and dorsal (**j**) sides. Black arrow indicates the acute anterior body end. **k**–**m** Details of the silverline pattern in the middle (**k**), anterior (**l**), and posterior (**m**) body portions. Red arrows indicate the short intermeridional connectives. *Explanations* = excretory pores (*EP*), macronucleus (*MA*), micronucleus (*MI*), paroral membrane (*Pa*), primary silverline meridian (*PM*), secondary silverline meridian (*SM*), somatic kineties (*SK*), adoral membranelles 1–3 (*M1*–*M3*). *Scale bars* = 7 μm (**c**, **g**, **h**, **k**–**m**) and 20 μm (**a**, **b**, **d**, **e**, **f**, **i**, **j**)

Type locality: River Hornád near the village of Milhosť, Slovakia (N 48° 31′ 45″, E 21° 18′ 20″).

Type host: *Unio tumidus* Philipsson, 1788.

Type material: A DNA sample of holotype specimen has been deposited in Natural History Museum, Vajánskeho nábrežie 2, 810 06 Bratislava, Slovakia (ID Collection Code 01427608).

Table 3 Morphometric data on *Tetrahymena foissneri* sp. n. (upper line) and *Tetrahymena unionis* sp. n. (lower line)

Character[a]	Mean	M	SD	SE	CV	Min	Max	*n*
Body, length	33.3	34.0	7.5	1.3	22.6	20.0	46.0	35
	41.8	39.5	7.0	1.3	16.8	26.0	56.0	30
Body, length (silver nitrate impregnation)	37.7	38.0	5.4	0.9	14.2	25.0	49.0	35
	48.1	47.0	6.9	1.0	14.5	35.0	62.0	51
Body, width	21.6	22.0	3.7	0.6	17.3	15.0	28.0	35
	25.4	24.0	4.0	0.7	15.7	20.0	33.0	30
Body, width (silver nitrate impregnation)	24.9	25.0	4.8	0.8	19.2	12.0	31.0	35
	36.6	36.0	6.1	0.9	16.7	24.0	51.0	51
Body length:width, ratio	1.5	1.5	0.1	0.0	9.0	1.3	1.8	35
	1.7	1.6	0.2	0.0	13.9	1.2	2.4	30
Body length:width, ratio (silver nitrate impregnation)	1.6	1.5	0.3	0.1	19.3	1.2	2.2	35
	1.3	1.3	0.1	0.0	9.6	1.1	1.6	51
Anterior body end to anterior end of macronucleus, distance	12.3	13.0	4.8	0.9	38.7	4.5	18.6	35
	15.5	15.3	3.2	0.6	20.7	5.2	22.0	29
Macronucleus, largest diameter	12.3	12.0	2.0	0.4	16.7	6.0	3.0	35
	17.0	16.5	2.6	0.5	15.5	12.3	22.6	29
Micronucleus, largest diameter	2.7	2.6	0.4	0.1	14.0	2.2	3.5	16
	3.2	3.0	0.8	0.4	26.3	2.3	4.4	5
Anterior body end to posterior end of buccal cavity, distance	13.1	13.5	2.2	0.4	16.6	8.0	16.6	35
	14.0	14.0	2.2	0.4	15.7	7.7	16.7	29
Oral apparatus, length (silver nitrate impregnation)	7.2	7.2	0.4	0.2	5.2	6.7	7.7	6
	12.5	13.0	1.3	0.3	10.8	8.0	15.0	27
Oral apparatus, % of body length (silver nitrate impregnation)	19.2	19.0	1.8	0.8	9.3	16.8	22.6	6
	26.1	26.0	3.3	0.7	12.7	20.5	33.3	27
Anterior body end to beginning of paroral membrane, distance	6.9	6.7	1.2	0.2	17.1	4.4	8.9	26
	5.1	4.8	2.0	0.4	39.1	1.4	11.7	28
Paroral membrane, length[b]	7.0	7.3	1.1	0.2	15.0	5.3	8.8	26
	8.9	8.9	1.2	0.2	13.0	6.4	11.9	28
Anterior body end to beginning of membranelle M1, distance	5.7	5.7	1.3	0.2	21.9	3.0	8.4	26
	3.6	3.8	1.2	0.2	33.7	0.8	6.7	28
First adoral membranelle (M1), length	3.7	3.7	0.7	0.1	17.9	2.1	4.6	26
	7.2	7.1	0.9	0.2	12.6	5.3	9.6	28
Second adoral membranelle (M2), length	3.3	3.3	0.7	0.1	19.9	2.0	4.4	26
	5.8	5.7	0.8	0.2	14.6	3.7	7.5	28
Third adoral membranelle (M3), length	2.0	2.0	0.3	0.1	16.8	1.2	2.8	26
	2.1	2.2	0.4	0.1	18.3	1.3	3.1	28
Somatic kineties, number	29.4	30.0	2.8	0.7	9.4	25.0	34.0	16
	28.2	28.0	2.4	0.7	8.4	24.0	33.0	11
Postoral kineties, number	2.9	3.0	0.3	0.1	10.9	2.0	3.0	16
	1.9	2.0	0.3	0.1	15.1	1.0	2.0	11
Kinetids in a dorsal kinety, number	29.6	29.5	3.2	0.9	10.8	24.0	34.0	16
	35.4	35.0	5.4	1.7	15.3	26.0	47.0	11

[a] Data based, if not mentioned otherwise, on mounted, protargol-impregnated, and randomly selected specimens. Measurements in μm. *Explanations* = coefficient of variation in % (*CV*), median (*M*), maximum (*Max*), arithmetic mean (*Mean*), minimum (*Min*), number of individuals investigated (*n*), standard deviation (*SD*), standard error of arithmetic mean (*SE*)

[b] Measured from the anterior to the posterior end, i.e., not following the curvature of the paroral membrane

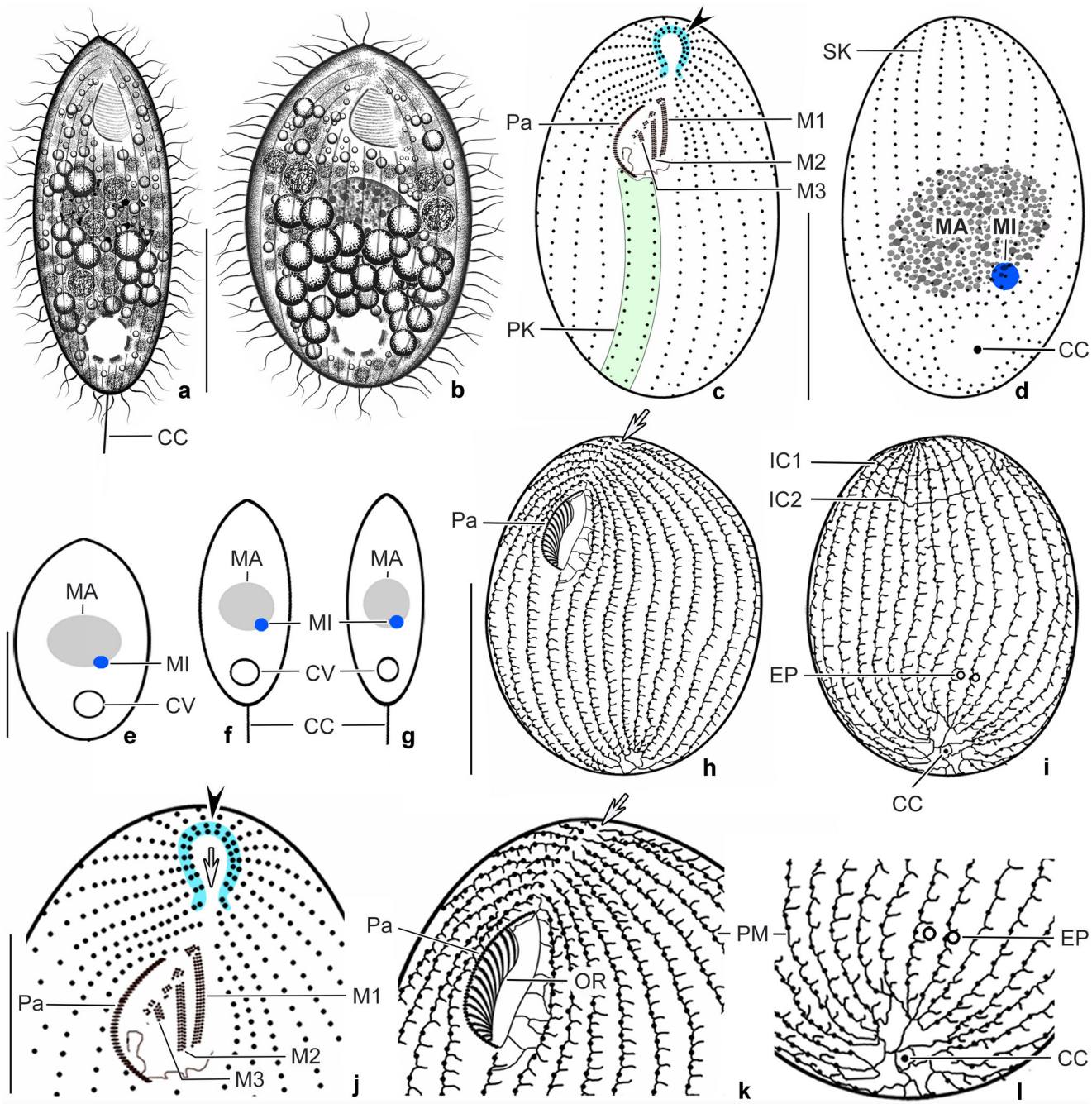

Fig. 4 *Tetrahymena unionis* sp. n. from life (**a**, **b**, **e**–**g**), after protargol impregnation (**c**, **d**, **j**), and after dry silver nitrate impregnation (**h**, **i**, **k, l**). **a**, **b** Ventral overviews, showing two different body shapes. **c**, **d** Ciliary pattern and nuclear apparatus of the ventral (**c**) and dorsal (**d**) sides. Black arrowhead marks dikinetids at the anterior end of the ciliary rows (blue area). **e**–**g** Overviews, showing the variability of body shape and size, the contractile vacuoles as well as the nuclear apparatus, which consists of one macronuclear nodule (shaded grey) and a single micronucleus (shaded blue). Drawn to scale. **h**, **i** Ciliary and silverline pattern of the ventral (**h**) and lateral (**i**) sides. White arrow in (**h**) shows the preoral suture. **j**–**l** Details of the anterior (**j**, **k**) and posterior (**l**) body portions. Black arrowhead marks dikinetids at the beginning of the ciliary rows (blue area), white arrow shows the preoral suture. *Explanations* = caudal cilium (*CC*), contractile vacuole (*CV*), excretory pores (*EP*), intermeridional silverline connectives (*IC1, IC2*), macronucleus (*MA*), micronucleus (*MI*), oral ribs (*OR*), paroral membrane (*Pa*), postoral kineties (*PK*), primary silverline meridian (*PM*), somatic kineties (*SK*), adoral membranelles 1–3 (*M1–M3*). *Scale bars* = 12 μm (**j–l**) and 20 μm (**a–i**)

Additional material: One paratype slide containing protargol-impregnated specimens (reg. no. 2021/3-ZTY) and one paratype slide containing silver nitrate-impregnated specimens (reg. no. 2021/4-ZTY) have been deposited at Department of Zoology, Comenius University in Bratislava, Ilkovičova 6, 842 15 Bratislava, Slovakia.

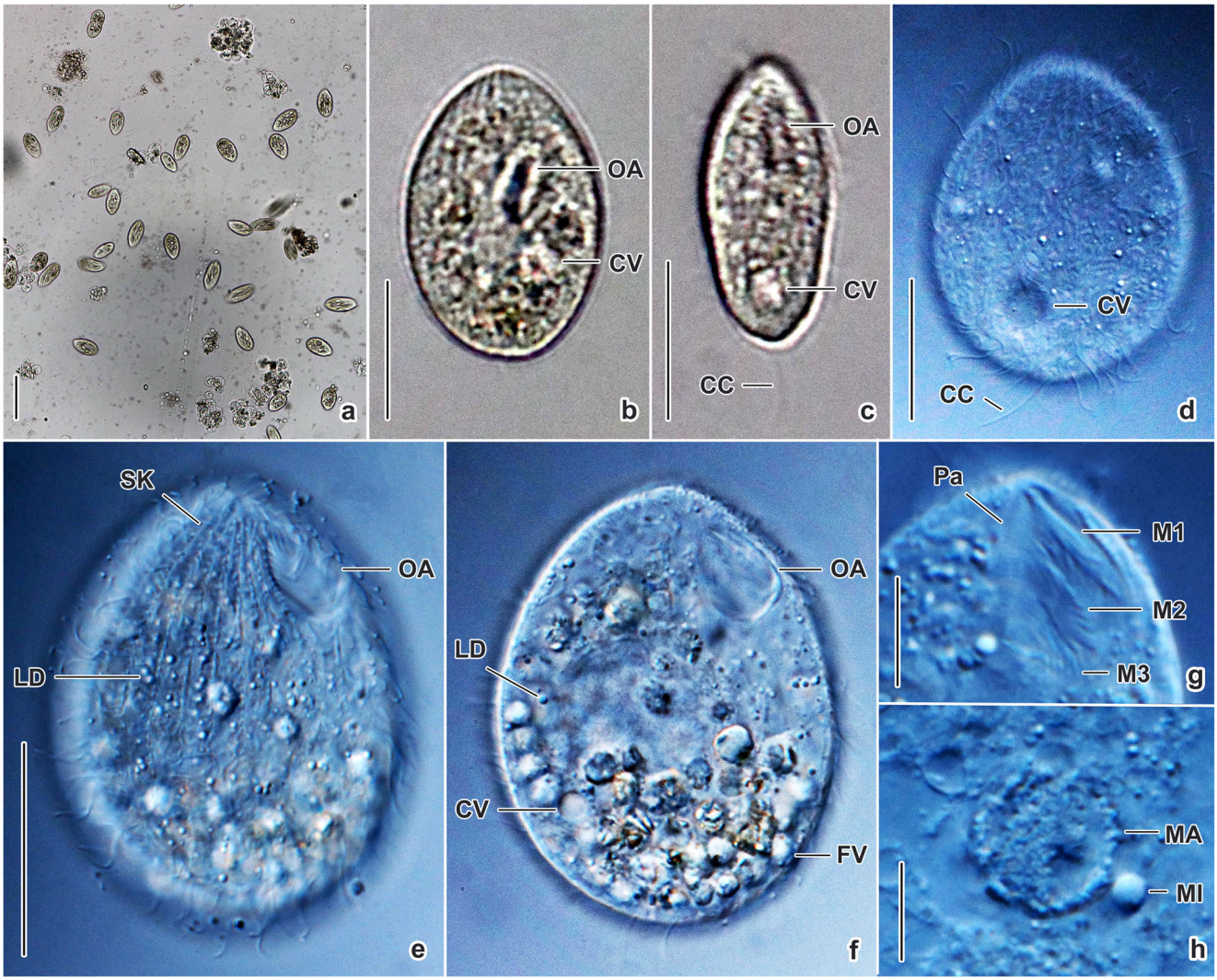

Fig. 5 *Tetrahymena unionis* sp. n. from life. **a** Overview, showing many cells expelled from the mantle cavity by *Unio tumidus* after exposure to tap water. **b**, **c** Ventral views of representative specimens, showing the two contrasting body shapes, the contractile vacuoles, and the oral apparatus. **d**–**f** Dorsal (**d**) and ventrolateral (**e**, **f**) overviews, showing the caudal cilium, contractile vacuole, oral apparatus, somatic kineties, and cytoplasmic inclusions. **g**, **h** Details of the oral (**g**) and nuclear (**h**) apparatus. *Explanations* = caudal cilium (*CC*), contractile vacuole (*CV*), food vacuoles (*FV*), lipid droplets (*LD*), macronucleus (*MA*), micronucleus (*MI*), oral apparatus (*OA*), paroral membrane (*Pa*), somatic kineties (*SK*), adoral membranelles 1–3 (*M1*–*M3*). *Scale bars* = 8 μm (**g**, **h**), 20 μm (**b**–**f**), and 100 μm (**a**)

Gene sequences: The nuclear 18S rRNA gene, the mitochondrial 16S rRNA gene, and the mitochondrial cytochrome *c* oxidase subunit I sequences of the holotype specimen have been deposited in GenBank (https://www.ncbi.nlm.nih.gov/genbank/) under the following accession nos. MW827181, MW827190, and MW828688, respectively.

Etymology: The specific epithet is a singular genitive case of the Latin noun *unio*, *union·is* [f], meaning a *Tetrahymena* from *Unio*. The species-group name is to be treated as an adjective used as a substantive in the genitive case, because of its derivation from the host's generic name (Art. 11.9.1.4. of the International Commission on Zoological Nomenclature 1999).

Description: Body size in vivo approximately 35–65 × 18–40 μm, with a length:width ratio of about 1.3–2.7:1 (n = 8). Shape narrowly elliptical to broadly ovate, anterior end slightly tapered, posterior end narrowly to broadly rounded; flexible but not contractile (Figs. 4a, b, e–g and 5a–c). Macronucleus usually located in body center, globular to ellipsoidal, on average 17 μm in largest diameter after protargol impregnation; innumerable circular nucleoli evenly distributed over macronucleus. A single micronucleus typically attached to posterior side of macronucleus, globular and about 2.3–4.4 μm across after protargol impregnation (Figs. 4a, b, d–g; 5h; 6a–f, j; and Table 3). One contractile vacuole situated dorsally and distinctly subterminally, about 4.5–7.0 μm in diameter during diastole; two interkinetal excretory pores each situated slightly right of ciliary rows (Figs. 4i, l and 6h). Cytoplasm colorless, contains numerous lipid droplets about 0.5 μm across and some to many food vacuoles up to 5.5 μm in

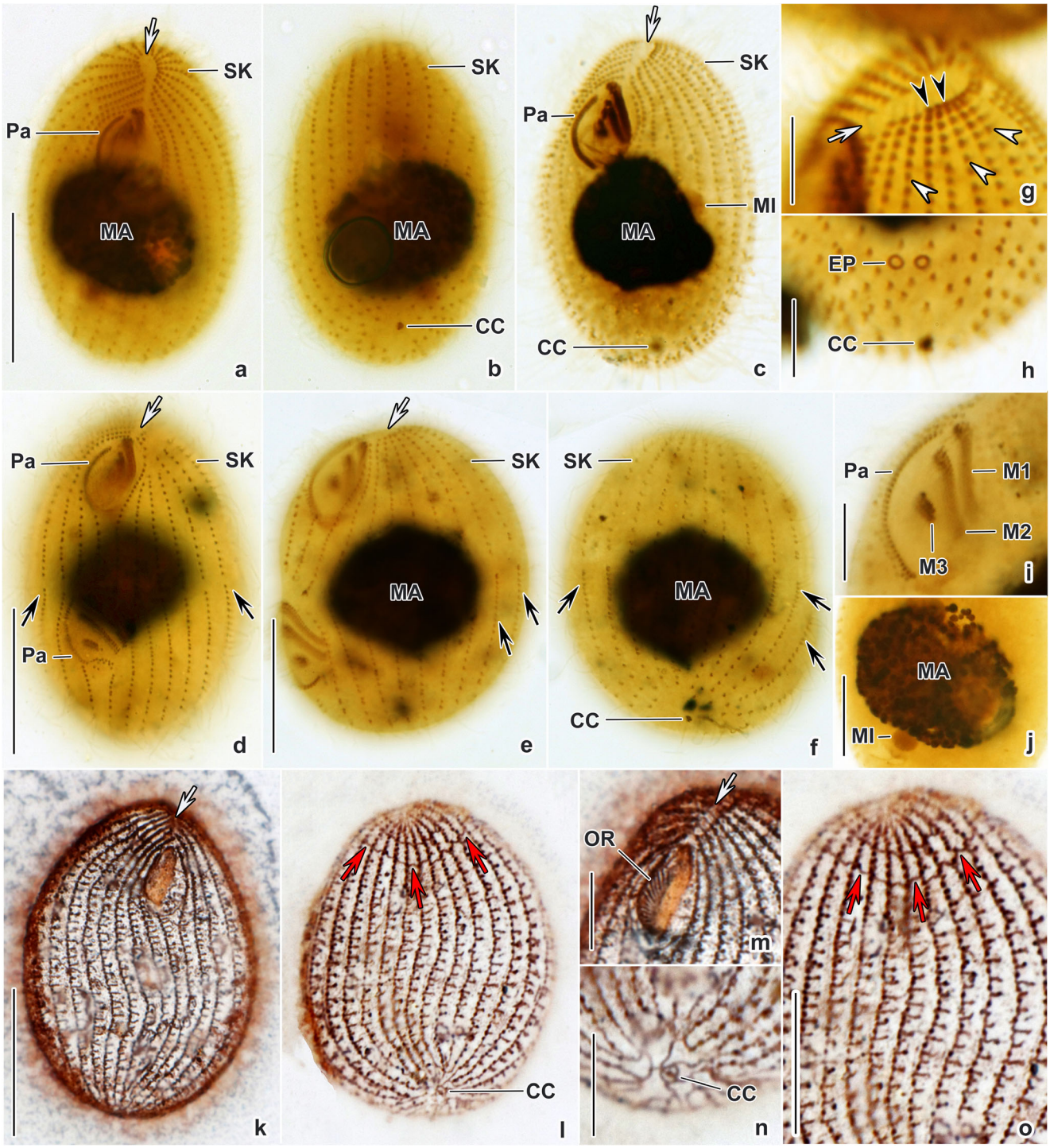

Fig. 6 *Tetrahymena unionis* sp. n. after protargol (**a**–**j**) and dry silver nitrate (**k**–**o**) impregnation. **a**–**c** Ciliary pattern and nuclear apparatus of the ventral (**a, c**) and dorsal (**b**) sides of representative specimens. White arrows mark the preoral suture. **d**–**f** Ciliary pattern and nuclear apparatus of mid-dividers. Black arrows show the broken somatic kineties, white arrows indicate the preoral suture. **g, i** Details of the anterior body end (**g**) and oral apparatus (**i**). Black arrowheads in (**g**) mark dikinetids at the anterior end of the ciliary rows, white arrowheads denote the monokinetids, white arrow indicates the preoral suture. **h** Detail of the posterior body portion, showing the excretory pores of the contractile vacuole and the basal body of the caudal cilium. **j** Detail of the nuclear apparatus. **k**, **l** Overviews of the silverline system on the ventral (**k**) and dorsal (**l**) sides. White arrow marks the preoral suture, red arrows show the intermeridional connectives. **m**–**o** Details of the ventral (**m**) and dorsal (**o**) sides of the anterior body portion, as well as of the posterior body end (**n**). White arrow marks the preoral suture, red arrows show the intermeridional connectives. *Explanations* = caudal cilium (*CC*), excretory pores (*EP*), macronucleus (*MA*), micronucleus (*MI*), oral ribs (*OR*), paroral membrane (*Pa*), somatic kineties (*SK*), adoral membranelles 1– 3 (*M1–M3*). *Scale bars* = 6 μm (**g**–**j**), 8 μm (**m**–**o**), and 20 μm (**a**–**f**, **k**, **l**)

diameter and usually containing pieces of host tissues (Figs. 4a, b and 5e, f). Cortex flexible, no cortical granules recognizable. Locomotion by slowly swimming while rotating about longitudinal body axis or rarely by gliding on the bottom of Petri dish. Feeds on host tissues and possibly also on bacteria in cultures.

Somatic cilia about 5.5–7.5 μm long in vivo, distinctly more densely spaced anteriorly than posteriorly, arranged in 24–33 meridional rows (Table 3). Ciliary pattern similar to that of previous species: (i) typically two postoral ciliary rows, (ii) ventral ciliary rows begin from almost anterior body end to mid-portion of oral apparatus and run right and left of buccal cavity, (iii) lateral and dorsal ciliary rows commence subapically leaving a small, horseshoe-shaped unciliated apical area, (iv) an indistinct and short suture anterior to oral apparatus, (v) all ciliary rows composed entirely from monokinetids, except for lateral and dorsal kineties which begin with a dikinetid each (Figs. 4a–d, h–l; 5d, e; and 6a–g, k–o). Caudal cilium stiff and conspicuously longer than ordinary somatic cilia, i.e., about 11 μm long in vivo, seen in all slender specimens investigated in detail (Figs. 4a, f, g and 5c, d) but not in well fed cells (Fig. 4b, e), very likely lost during manipulation as the basal body of caudal cilium was observed in slender and broad specimens after protargol impregnation (Figs. 4d and 6b, c, f, h) and dry silver nitrate impregnation (Figs. 4i, l and 6l, n).

Silverline system composed of only primary meridians extending within somatic ciliary rows. Conspicuous outgrowths (peaks) emerge on left side of primary meridians between each two kinetids. Two intermeridional silverlines transversely connect right and left ciliary rows of dorsal side in anterior body portion, possibly transverse intermeridional silverlines also on ventral side but too faintly impregnated and thus difficult to recognize. All posterior basal bodies radiate silverlines to make a circle around basal body of caudal cilium (Figs. 4h, i, k, l and 6k–o).

Oral apparatus situated in a relatively deep cavity of ventral body side, i.e., in about anterior fifth of body length, ca. 8–15 μm long after dry silver nitrate impregnation (Table 3). Oral ciliature as usual in tetrahymenids, i.e., composed of a paroral membrane and three membranelles. Paroral membrane J-shaped and composed of very narrowly spaced dikinetids. Membranelle M1 approximately 7.2 μm long, membranelle M2 about 5.8 μm long, and membranelle M3 only ca. 2.1 μm long after protargol impregnation; each membranelle composed of three almost equally long rows of basal bodies (Table 3). Patches of irregularly arranged basal bodies right of membranelles in some specimens, very likely reorganizing postdividers. Cytopharyngeal fibers originate from basal bodies of paroral membrane, extend towards midline of oral cavity, well recognizable in some silver nitrate-impregnated specimens, only weakly impregnated with the protargol method used (Figs. 4a–c, h, j, k; 5b, c, e–g; and 6a, c, i, k, m).

Notes on division: Although only few mid-dividers were found in the protargol slides, they document that the ontogenesis of *T. unionis* follows the tetrahymenid mode. More specifically, binary fission is homothetogenic (i.e., the main body axes of the proter and the opiste have the same orientation) and occurs in freely motile condition. Stomatogenesis is monoparakinetal, that is, the rightmost postoral kinety produces the oral anlage of the opisthe. The parental oral structures are not involved in the formation of the daughter oral ciliature and are not reorganized. In mid-dividers, the somatic ciliary rows split in the middle leaving a barren area at the posterior region of the proter and at the anterior region of the opisthe (Fig. 6f, h).

Prevalence and intensity: *T. unionis* was detected in all five *Unio tumidus* specimens collected from the type locality. Although all mussels were heavily colonized with ciliates (more than five hundred individuals per mussel), no signs of pathological changes were detected. Despite our research on multiple native (*Anodonta anatina*) and invasive mussel species (*Corbicula fluminea*, *Dreissena polymorpha*, *Sinanodonta woodiana*), tetrahymenids were not detected in them. Likewise, no tetrahymenids were found in native (*Theodoxus danubialis*, *Viviparus contectus*) and invasive (*Potamopyrgus antipodarum*) aquatic pulmonate mollusks. *Tetrahymena unionis* is thus very likely a rare species.

Phylogenetic analyses

Altogether, 27 new sequences of three molecular markers (16S, 18S rRNA, and COI genes) were obtained from *T. foissneri* sp. n. and *T. unionis* sp. n. Their GenBank accession numbers, length, and guanine-cytosine content are summarized in Table 4. Three different algorithms (maximum likelihood, Bayesian inference, and neighbor-joining) were used to determine the phylogenetic positions of the two new *Tetrahymena* species, using the 16S and 18S rRNA as well as the COI gene sequences (Figs. 7, 8, and 9 and Suppl. Fig. S1). Although the overall tree topologies slightly differed depending on the molecular marker(s) and taxon sampling, *T. foissneri* and *T. unionis* were consistently classified within the same clades across all phylogenetic analyses. Specifically, *T. foissneri* was depicted within the '*borealis*' clade in a sister position to *T. limacis* with full statistical support in the COI trees (Fig. 8) as well as in the 18S rRNA gene + COI trees (Fig. 7). As no 16S rRNA gene sequences are available for *T. limacis*, *T. foissneri* was left as an orphan lineage within the '*borealis*' clade in the 16S rRNA gene trees (Fig. 9) as well as in the 16S rRNA gene + COI trees (Suppl. Fig. S1).

Tetrahymena unionis was placed within the '*paravorax*' clade with full statistical support in all analyses (Figs. 7, 8, and 9 and Suppl. Fig. S1). *Tetrahymena pennsylvaniensis* isolated from freshwater, *T. glochidiophila* isolated from glochidia of freshwater mussels, and *T. nigricans* isolated from freshwater planarians were revealed as the nearest relatives of *T. unionis* with maximum statistical support. Phylogenetic relationships among these four species were, however, not well resolved either in the single-

Table 4 Characterization of new sequences of *Tetrahymena foissneri* sp. n. and *Tetrahymena unionis* sp. n.

Specimen	18S rRNA gene			16S rRNA gene			Cytochrome *c* oxidase subunit I		
	Length (nt)	GC (%)	GenBank entry	Length (nt)	GC (%)	GenBank entry	Length (nt)	GC (%)	GenBank entry
T. foissneri ST 1 AV[a]	1712	42.99	MW827176	1001	27.87	MW827185	945	25.29	MW828683
T. foissneri ST 2 AV	1712	42.99	MW827177	1001	27.87	MW827186	945	25.29	MW828684
T. foissneri ST 3 AV	1712	42.99	MW827178	1001	27.87	MW827187	945	25.29	MW828685
T. foissneri ST 4 AV	1712	42.99	MW827179	1001	27.87	MW827188	945	25.29	MW828686
T. foissneri ST 5 AV	1712	42.99	MW827180	1001	27.87	MW827189	945	25.29	MW828687
T.unionis HO 35 UT[b]	1707	43.06	MW827181	1009	31.32	MW827190	945	27.20	MW828688
T.unionis HO 37 UT	1707	43.06	MW827182	1009	31.32	MW827191	945	27.20	MW828689
T.unionis HO 38 UT	1707	43.06	MW827183	1009	31.32	MW827192	945	27.20	MW828690
T.unionis HO 39 UT	1707	43.06	MW827184	1009	31.32	MW827193	945	27.20	MW828691

[a] Genomic DNA of the holotype specimen of *T. foissneri* has been deposited in Natural History Museum in Bratislava, Slovakia (ID Collection Code 01427572)

[b] Genomic DNA of the holotype specimen of *T. unionis* has been deposited in Natural History Museum in Bratislava, Slovakia (ID Collection Code 01427608)

gene or in the two-gene trees. To further address this problem, 18S rRNA and COI gene sequences of these four species were analyzed using the Bayesian coalescent approach, which accounts for ancestral polymorphism and incomplete lineage sorting. Bayesian coalescent analyses delimited all four *Tetrahymena* species with a posterior probability of 1.00. Moreover, *T. glochidiophila* was recognized to be sister to *T. nigricans* with full statistical support. However, the phylogenetic position of *T. unionis* remained unresolved also in the coalescent species trees, as it was depicted sister to the *T. pennsylvaniensis*, *T. glochidiophila*, and *T. nigricans* cluster but with a negligible posterior probability of 0.52 (not shown).

Discussion

Erection of two new *Tetrahymena* species

To establish new ciliate species, Warren et al. (2017) recommended preparing detailed morphological descriptions and taxonomic analyses of relevant distinguishing diagnostic characters. However, most *Tetrahymena* species have a rather similar body shape and size as well as overlapping numbers of ciliary rows. The uniformity of the genus *Tetrahymena* makes the erection of new species based solely on morphological characteristics to be very difficult in practice (e.g., Lynn et al. 2018; Quintela-Alonso et al. 2013). Thus, following Doerder (2019) as well as Rataj and Vďačný (2020), three molecular markers (16S, 18S rRNA, and COI genes) were used to define and separate the two new tetrahymenid ciliates isolated from mollusks. According to Chantangsi et al. (2007), the COI gene is taxonomically most important, as tetrahymenid ciliates exhibit an average of about 10% interspecific genetic divergence while less than 1% intraspecific variability in the barcoding region of their COI sequences. Doerder (2014, 2019) applied a 4% interspecific divergence as a threshold for species delimitation using the barcoding region of the COI gene. We also considered the genetic comparison and especially the COI divergence as the most important part in the argumentation for the establishment of new *Tetrahymena* species.

Tetrahymena foissneri sp. n., which was isolated from the invasive Lusitanian slug *Arion vulgaris*, differs from its nearest relative *T. limacis* by 6.34% in the COI gene. On the other hand, their 18S rRNA gene sequences are identical and their 16S rRNA gene sequences share a 99.88% identity. The high similarity of the nuclear and mitochondrial rRNA genes indicates a close kinship of these two species parasitizing slugs. However, their taxonomic distinctness and species status are supported not only by COI gene sequences but also by three morphological traits. The parasitic-phase forms of *T. limacis* have an anterior body end differentiated into a conspicuous thorn (Kozloff 1946; Warren 1932), while the anterior end of freshly isolated, parasitic-phase forms of *T. foissneri* is acute and never apiculate (Figs. 1a, d–g; 2a–c; and 3i, j). Nonetheless, it is important to mention that the anterior end of *T. limacis* becomes acute after cultivation (Corliss 1973), causing that the body shape of the parasitic-phase forms of *T. foissneri* and the cultured forms of *T. limacis* to become highly similar. Therefore, the morphology of freshly isolated ciliates needs to be compared. Both species can be furthermore separated by the diameter of the micronucleus, which never exceeds 2.5 μm in *T. limacis* (Corliss 1973) but ranges from about 2.3 to 4.4 μm in *T. foissneri* (Table 3). Finally, *T. limacis* has three transverse intermeridional silverline connectives in the anterior body region (Kozloff 1946), which were never observed in *T. foissneri* (Figs. 1i, j and 3i, j, l).

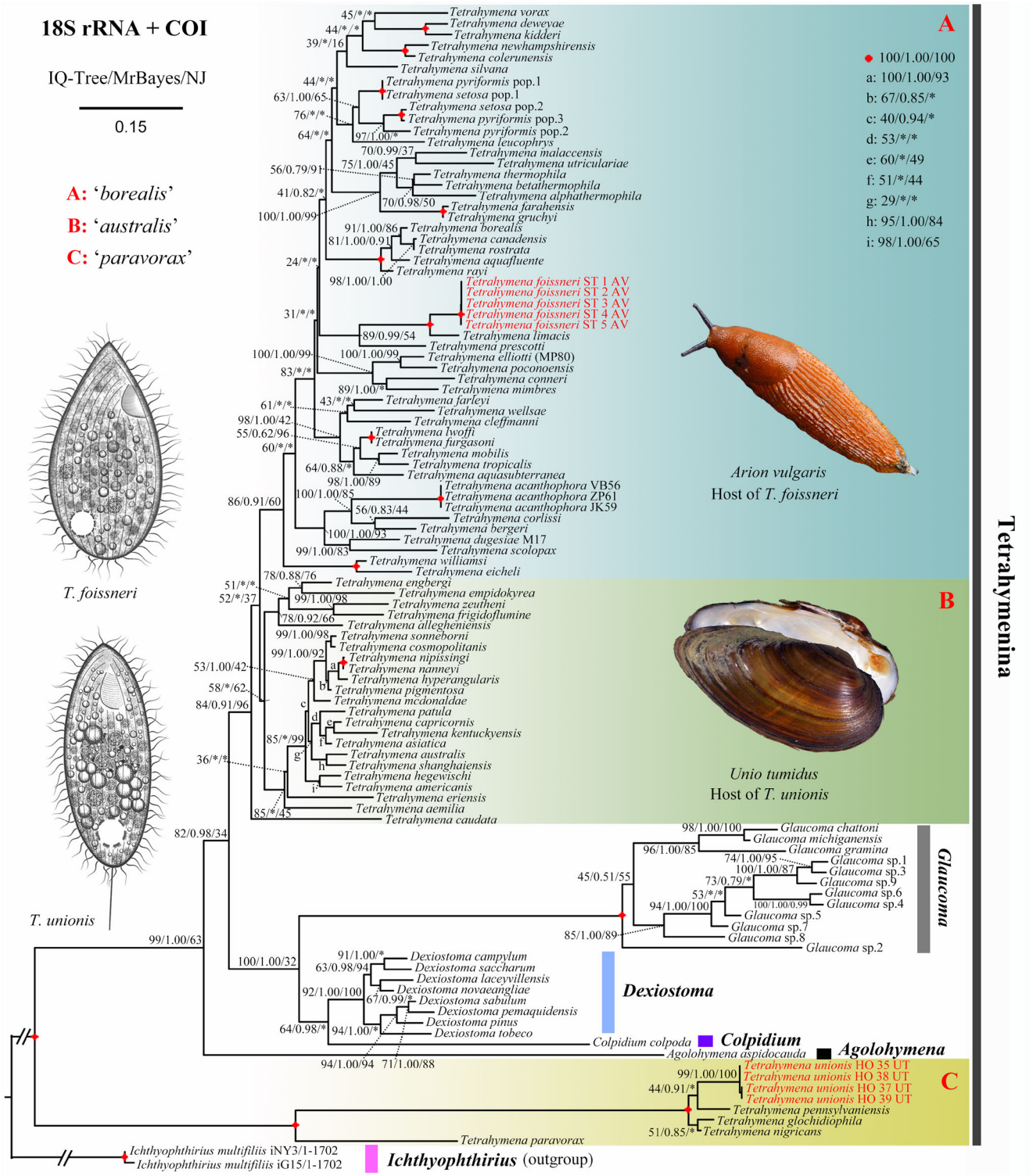

Fig. 7 Phylogenetic tree based on the nuclear 18S rRNA gene and the mitochondrial cytochrome *c* oxidase subunit I (COI) sequences, showing the systematic position of tetrahymenids newly isolated from mollusks. The genus *Ichthyophthirius* was used as an outgroup. Bootstrap values for maximum likelihood conducted in IQ-Trees, posterior probabilities for Bayesian inference conducted in MrBayes, and NJ bootstrap values were mapped onto the best scoring IQ-tree. Asterisks indicate a mismatch between maximum likelihood and Bayesian and/or NJ tree topologies. Sequences marked by red color were obtained during this study. Fully statistically supported nodes are marked with red solid circles. The strain MP80 was mislabeled as *T. elliotti* by Chantangsi et al. (2007). According to Doerder (2019), *T. elliotti* is related to *T. gruchyi*. GenBank accession numbers can be found in Supplementary Table S2. The scale bar represents the expected number of nucleotide substitutions per site

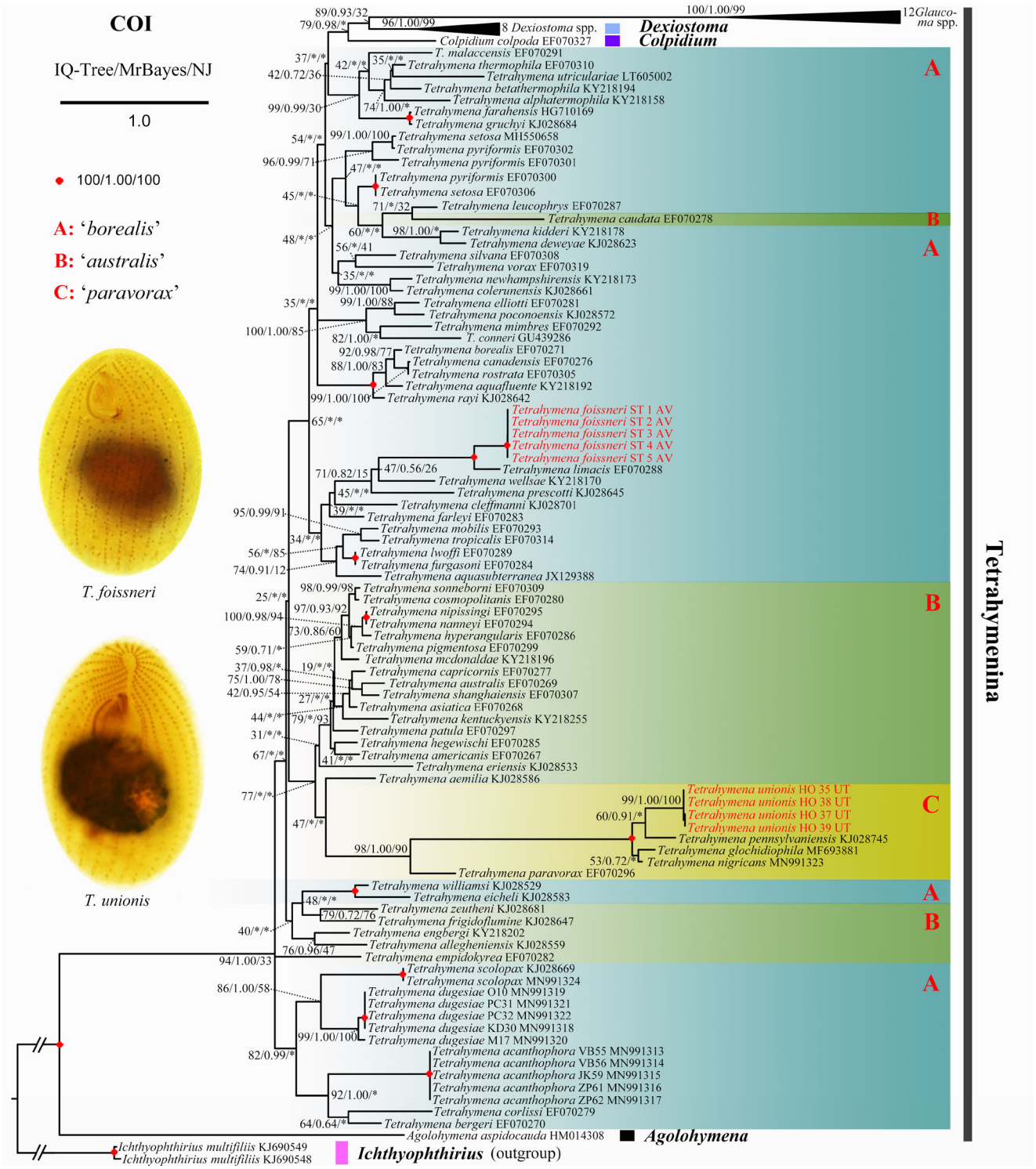

Fig. 8 Phylogenetic tree based on the mitochondrial COI sequences, showing the systematic position of tetrahymenids newly isolated from mollusks. The genus *Ichthyophthirius* was used as an outgroup. Bootstrap values for maximum likelihood conducted in IQ-Trees, posterior probabilities for Bayesian inference conducted in MrBayes, and NJ bootstrap values were mapped onto the best scoring IQ-tree. Asterisks indicate a mismatch between maximum likelihood and Bayesian and/or NJ tree topologies. Sequences marked by red color were obtained during this study. Fully statistically supported nodes are marked with red solid circles. The strain MP80 was mislabeled as *T. elliotti* by Chantangsi et al. (2007). The scale bar represents the expected number of nucleotide substitutions per site

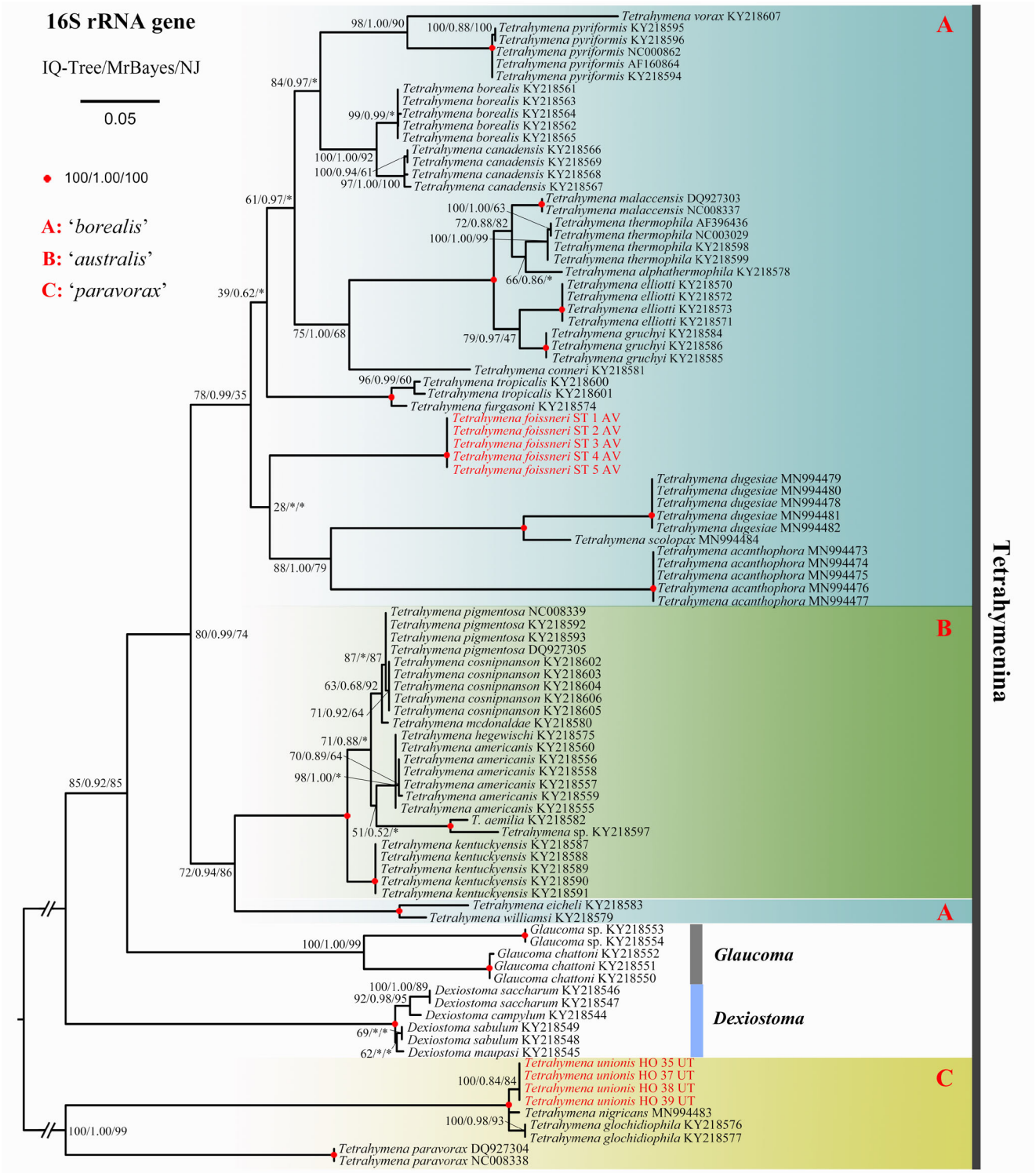

Fig. 9 Phylogenetic tree based on the mitochondrial 16S rRNA gene sequences, showing the systematic position of tetrahymenids newly isolated from mollusks. Bootstrap values for maximum likelihood conducted in IQ-Trees, posterior probabilities for Bayesian inference conducted in MrBayes, and NJ bootstrap values were mapped onto the best scoring IQ-tree. Asterisks indicate a mismatch between maximum likelihood and Bayesian and/or NJ tree topologies. Sequences marked by red color were obtained during this study. Fully statistically supported nodes are marked with red solid circles. The scale bar represents the expected number of nucleotide substitutions per site

Tetrahymena unionis n. sp., which originated from the swollen river mussel *Unio tumidus*, is closely related to *T. pennsylvaniensis*, *T. glochidiophila*, and *T. nigricans*, all belonging to the '*paravorax*' clade. The COI sequences of the new species differ from those of *T. pennsylvaniensis* by 8.29%, from *T. glochidiophila* by 7.51–7.56%, and from *T. nigricans* by 8.52%. *Tetrahymena unionis* shares a 99.82–99.88% identity in the 18S rRNA gene and a 98.42–99.19% identity in the 16S rRNA gene with its three nearest relatives. These genetic differences along with the present Bayesian coalescent delimitation analyses undoubtedly corroborate the species status of the new Slovak isolate. As there are no detailed morphological data on *T. pennsylvaniensis* (Doerder 2019), no comparison is possible. Although the morphological description of *T. nigricans* is very brief (Rataj and Vďačný 2020), the new species is much smaller (35–65 × 18–40 μm *vs*. 75–90 × 55–70 μm) and has a different body shape (narrowly elliptical to broadly ovate, anterior end slightly tapered, posterior end broadly to narrowly rounded *vs.* elliptical with both body ends broadly rounded). Moreover, *T. nigricans* originated from the invasive North American planarian *Girardia tigrina*, while *T. unionis* was isolated from a native bivalve *Unio tumidus*. Albeit the morphological description of Lynn et al. (2018) is very detailed, no relevant morphological distinguishing characters between *T. glochidiophila* and *T. unionis* were found. Thus, besides molecular data, the host organism might be so far considered as a further relevant difference. Specifically, the former species parasitizes glochidia of the genus *Lampsilis* (family Unionidae), while the latter species was isolated from adults of *Unio tumidus*. Additionally, the type locality of *T. glochidiophila* is in North America, while that of *T. unionis* in Central Europe. Nevertheless, much more research needs to be conducted whether host preference and the geographic place of origin might be counted among the relevant taxonomic differences.

Tetrahymena infections of mollusks

Only little attention has been paid to the diversity of tetrahymenids infecting mollusks in the past two decades. To date, only three *Tetrahymena* species have been reported from terrestrial gastropods, namely, *T. limacis* and *T. pyriformis* mostly from their digestive system, and *T. rostrata* mostly from their renal organ (for a review, see Van As and Basson 2004). With regard to aquatic mollusks, Dobrzańska (1958) recorded two *Tetrahymena* species in three bivalve species: *Pisidium casertanum*, *P. obtusale*, and *Sphaerium lacustre*. She identified them as *T. limacis* and *T. pyriformis*, which was, however, questioned by Corliss (1960) due to the lack of any morphological information. Since no DNA samples from these two tetrahymenid isolates are available, their identity cannot be tested with modern molecular methods. Very likely, the *T. pyriformis* of early studies of parasitism may not be the species *T. pyriformis* recognized today. To our best knowledge, the last reports of *Tetrahymena* infecting aquatic mollusks come from the bivalve *Lampsilis siliquoidea*, *L. fasciola*, and *L. cardium* (family Unionidae) whose glochidia are parasitized by *T. glochidiophila* (Lynn et al. 2018; Prosser et al. 2018). Despite our comparatively broad sampling (150 specimens belonging to six bivalve and 13 gastropod species), we detected tetrahymenids only twice. They could not be assigned to any of the aforementioned species parasitizing mollusks. Molecular analyses indicated that the first species, *T. foissneri*, is related to *T. limacis* from the '*borealis*' clade, and the other species, *T. unionis*, is related to *T. glochidiophila* from the '*paravorax*' clade. Although only 10.52% of the examined mollusk species were infected, we believe that a discovery of further new *Tetrahymena* species is to be expected with increased host sampling.

Van As and Basson (2004) very carefully reviewed records of terrestrial gastropods infected by *Tetrahymena* species. According to their list, wild populations of terrestrial gastropods rather commonly host *T. limacis* and *T. rostrata*, while *T. pyriformis* is considered a facultative parasite of gastropods, as it was able to infect the slug *Deroceras reticulatum* in experimental studies (Kozloff 1956a). Interestingly, the majority of reports of *Tetrahymena* infections come from the genus *Deroceras* (family Agriolimacidae) especially from *D. reticulatum*, which seems to be the most common host of *T. limacis* (Arias and Crowell 1963; Borden 1948; Brooks 1968; Kozloff 1946; Michelson 1971; Warren 1932; Windsor 1959). Further hosts of *T. limacis* are slugs of the families Arionidae, Milacidae, and Limacidae as well as snails of the families Bradybaenidae, Daudebardiidae, Helicidae, Hygromiidae, Succineidae, Vitrinidae, and Zonitidae (Brooks 1968; Kazubski 1958, 1959, 1960; Kazubski and Szablewski 1978; Kozloff 1956b).

Tetrahymena rostrata has a similarly long list of hosts and has been reported from the slug families Agriolimacidae, Arionidae, and Milacidae as well as from the snail families Clausiliidae, Cochlicopidae, Discidae, Oleacinidae, Valloniidae, Vitrinidae, and Zonitidae (Brooks 1968; Kazubski 1958, 1959, 1960; Kazubski and Szablewski 1978). This *Tetrahymena* species is also rather frequently encountered as a facultative parasite or a histophagous scavenger of other invertebrates. It is also readily found free-living in various edaphic habitats ranging from moss through leaf-litter to soil (e.g., Corliss 1973; Foissner 1998, 2000). On the other hand, *T. limacis* is edaphic only in the sense that it is occasionally found free-living in its host's environment (Corliss 1973). Unfortunately, we did not examine soil samples from the site where the host of *T. foissneri* was found and, therefore, we cannot exclude that it might also have a free-living phase.

It seems that *T. limacis* is much more specific for mollusks than *T. rostrata*. However, the broad host spectrum of both *Tetrahymena* species needs to be tested with molecular methods in the future, as morphology-based identification of tetrahymenids needs to be confirmed by genetic data. As *T. foissneri* has been recorded only once, its host specificity is open for further analyses of wild populations of gastropods. Nevertheless, *T. limacis* and *T. foissneri* appear to be ecologically more similar, as they have a strong affinity to the alimentary tract including the digestive gland, intestine, and rectum. On the other hand, *T. rostrata* apparently prefers the renal organ (Van As and Basson 2004; Segade et al. 2009).

Three possible routes of transmission of tetrahymenids to new mollusk hosts were speculated. Michelson (1971) suggested that transmission can occur through feces in the case of *T. limacis*, as it is able to produce resting cysts. Spreading via ingestion of fecal material contaminated by resting cysts would, in turn, enable a wide host range and low host specificity. Although we did not observe cyst formation in *T. foissneri*, its mass occurrence in the alimentary tract is also indicative that its transmission might be mediated by the fecal-oral route. Corliss (1973) speculated that the dorsal integumentary pouch might also serve as a portal of entry into an adult slug. In this case, transfer to new hosts might be facilitated by the gregarious behavior of slugs during feeding or breeding. Finally, trans-ovum transmission has been recorded for *T. rostrata* in *D. reticulatum* (Brooks 1968). Ciliates invade the albumen gland, which leads to their incorporation in eggs. Embryos became infected through ingestion during aspiration of the albumen. By contrast to the fecal-oral route, the trans-ovum transmission might result in high host specificity.

Although we did not observe any pathological effects of tetrahymenids associated with mollusks, high infections of *T. limacis* have fatal results on their gastropod hosts, especially when ciliates enter various internal organs including the kidney (Brooks 1968; Michelson 1971). *Tetrahymena rostrata* might be responsible for the density-dependent regulation in agriolimacids infesting lowland pastures (Barker 1993, 2002). According to experimental studies, it reduces the growth rate, feeding, and fecundity of its hosts (Van As and Basson 2004). Epizootic mortality in the natural populations of agriolimacids is very likely also mediated by the onset of hot weather in late spring to early summer (Barker 1993). Segade et al. (2009) also observed pathological effects of *T. rostrata* on snails. Specifically, their examinations of farmed helicid snails (*Helix aspersa aspersa* and *Helix aspersa maxima*) revealed a severe destruction of the renal epithelium in heavily infected hosts. There is also some evidence that *T. rostrata* may have further deleterious effects on *Helix aspersa*, i.e., swelling of the mantle collar and a marked inability to retract the body into the shell. Mantle swelling was observed also in *Deroceras reticulatum* infected experimentally with *T. rostrata* (Brooks 1968).

With regard to bivalves, the viability of glochidia is comparatively strongly affected by tetrahymenids. Their viability declined by more than 60% after exposition to *T. glochidiophila* for 72 h (Prosser et al. 2018). Despite this fact, *T. glochiophila* very likely does not have a significant effect on the reproduction of *Lampsilis* species in the wild, as the 24-h window of glochidia infectivity upon release from the marsupia may be too short for ciliates to develop high abundances. However, as *T. glochidiophila* has been found also free-living, there might be a pool of ciliates that can infect glochidia and hence further negatively affect the bivalve reproduction. Unfortunately, we did not examine water samples from the site where the host of *T. unionis* was found and, therefore, we cannot exclude that it might also have a free-living phase.

Supplementary Information The online version contains supplementary material available at https://doi.org/10.1007/s00436-021-07152-5.

Acknowledgements We are grateful to Daniel Gruľa and Matej Rataj for providing us the mussel samples, to Matej Rataj for sharing his datasets, and to Ivan Rúrik for his help with some bioinformatics tools.

Funding This work was supported by the Slovak Research and Development Agency under contract no. APVV-19-0076 and by the Grant Agency of the Ministry of Education, Science, Research and Sport of the Slovak Republic and Slovak Academy of Sciences under grant VEGA 1/0013/21.

Declarations

All applicable institutional, national, and international guidelines for the care and use of animals were followed.

Conflict of interest The authors declare no competing interests.

References

Antipa GA, Small EB (1971) The occurrence of thigmotrichous ciliated protozoa inhabiting the mantle cavity of unionid molluscs of Illinois. Trans Am Microsc Soc 90:463–472. https://doi.org/10.2307/3225461

Arias RO, Crowell HH (1963) A contribution to the biology of the gray garden slug. Bull South Calif Acad Sci 62:83–97 https://scholar.oxy.edu/handle/20.500.12711/10753

Barker GM (1993) Population regulation of *Deroceras* slugs (Agriolimacidae) in northern New Zealand pastures with particular reference to the role of *Tetrahymena rostrata* (Kahl) (Ciliata) and *Microsporidium novacastriensis* (Jones & Selman) (Microspora). In: Proceedings of the 3rd International Congress of Medical and Applied Malacology, 18–22 October 1993. Camden.

Barker GM (2002) Gastropods as pests in New Zealand pastoral agriculture, with emphasis on Agriolimacidae, Arionidae and Milacidae. In: Barker GM (ed) Molluscs as Crop Pests. CABI Publishing, Wallingford, pp 361–421

Batson BS (1983) *Tetrahymena dimorpha* sp. nov. (Hymenostomatida: Tetrahymenidae), a new ciliate parasite of Simuliidae (Diptera) with potential as a model for the study of ciliate morphogenesis. Philos Trans R Soc Lond B 301:345–363. https://doi.org/10.1098/rstb.1983.0027

Batson BS (1985) A paradigm for the study of insect-ciliate relationships: *Tetrahymena sialidos* sp. nov. (Hymenostomatida: Tetrahymenidae), parasite of larval *Sialis lutaria* (Linn.) (Megaloptera: Sialidae). Philos Trans R Soc Lond B 310:123–144. https://doi.org/10.1098/rstb.1985.0102

Borden VC (1948) Ciliates from *Deroceras agreste*. University of Virginia, Diploma Thesis

Bouckaert R, Heled J, Kühnert D, Vaughan T, Wu C-H, Xie D, Suchard MA, Rambaut A, Drummond AJ (2014) BEAST 2: a software platform for Bayesian evolutionary analysis. PLoS Comput Biol 10: e1003537. https://doi.org/10.1371/journal.pcbi.1003537

Brooks WM (1968) Tetrahymenid ciliates as parasites of the gray garden slug. Hilgardia 39:205–276. https://doi.org/10.3733/hilg.v39n08p205

Chantangsi C, Lynn DH, Brandl MT, Cole JC, Hetrick N, Ikonomi P (2007) Barcoding ciliates: a comprehensive study of 75 isolates of the genus *Tetrahymena*. Int J Syst Evol Microbiol 57:2412–2425. https://doi.org/10.1099/ijs.0.64865-0

Corliss JO (1960) *Tetrahymena chironomi* sp. nov., a ciliate from midge larvae, and the current status of facultative parasitism in the genus *Tetrahymena*. Parasitology 50:111–153. https://doi.org/10.1017/s0031182000025245

Corliss JO (1969) An up-to-date analysis of the systematics of the ciliate genus *Tetrahymena*. J Protozool 16:6–7. https://doi.org/10.1111/j.1550-7408.1969.tb04358.x

Corliss JO (1970) The comparative systematics of species comprising the hymenostome ciliate genus *Tetrahymena*. J Protozool 17:198–209. https://doi.org/10.1111/j.1550-7408.1970.tb02356.x

Corliss JO (1973) History, taxonomy, ecology, and evolution of species of *Tetrahymena*. In: Elliott AM (ed) Biology of *Tetrahymena*. Dowden, Hutchinson & Ross, Stroudsburg, PA, pp 1–55

Darriba D, Taboada GL, Doallo R, Posada D (2012) jModelTest 2: more models, new heuristics and parallel computing. Nat Methods 9:772. https://doi.org/10.1038/nmeth.2109

Dobrzańska J (1958) Investigations on ciliates living in lamellibranchiates of small water bodies. Bull Acad Polon Sci 6: 113–118

Doerder FP (2014) Abandoning sex: multiple origins of asexuality in the ciliate *Tetrahymena*. BMC Evol Biol 14:112. https://doi.org/10.1186/1471-2148-14-112

Doerder FP (2019) Barcodes reveal 48 new species of *Tetrahymena*, *Dexiostoma*, and *Glaucoma*: phylogeny, ecology, and biogeography of new and established species. J Eukaryot Microbiol 66:182–208. https://doi.org/10.1111/jeu.12642

Edgerton B, O'Donoghue P, Wingfield M, Owens L (1996) Systemic infection of freshwater crayfish *Cherax quadricarinatus* by hymenostome ciliates of the *Tetrahymena pyriformis* complex. Dis Aquat Org 27:123–129. https://doi.org/10.3354/dao027123

Ferguson HW, Hicks BD, Lynn DH, Ostland VE, Bailey J (1987) Cranial ulceration in Atlantic Salmon *Salmo salar* associated with *Tetrahymena* sp. Dis Aquat Org 12:191–195. https://doi.org/10.3354/dao002191

Foissner W (1987) Neue terrestrische und limnische Ciliaten (Protozoa, Ciliophora) aus Österreich und Deutschland. Sber Akad Wiss Wien 195:217–268

Foissner W (1998) An updated compilation of world soil ciliates (Protozoa, Ciliophora), with ecological notes, new records, and descriptions of new species. Eur J Protistol 34:195–235. https://doi.org/10.1016/S0932-4739(98)80028-X

Foissner W (2000) A compilation of soil and moss ciliates (Protozoa, Ciliophora) from Germany, with new records and descriptions of new and insufficiently known species. Eur J Protistol 36:253–283. https://doi.org/10.1016/S0932-4739(00)80003-6

Foissner W (2014) An update of 'basic light and scanning electron microscopic methods for taxonomic studies of ciliated protozoa'. Int J Syst Evol Microbiol 64:271–292. https://doi.org/10.1099/ijs.0.057893-0

Furgason WH (1940) The significant cytostomal pattern of the "*Glaucoma-Colpidium* group," and a proposed new genus and species, *Tetrahymena geleii*. Arch Protistenkd 94:224–266

Hall TA (1999) BioEdit: a user-friendly biological sequence alignment editor and analysis program for Windows 95/98/NT. Nucleic Acids Symp Ser 41:95–98

Hatai K, Chukanhom K, Lawhavinit OA, Hanjavanit C, Kunitsune M, Imai S (2001) Some biological characteristics of *Tetrahymena corlissi* isolated from guppy in Thailand. Fish Pathol 36:195–199. https://doi.org/10.3147/jsfp.36.195

Hoang DT, Chernomor O, von Haeseler A, Minh BQ, Vinh LS (2018) UFBoot2: improving the ultrafast bootstrap approximation. Mol Biol Evol 35:518–522. https://doi.org/10.1093/molbev/msx281

Hoffman GL, Landolt M, Camper JE, Coats DW, Stookey JL, Burek JD (1975) A disease of freshwater fishes caused by *Tetrahymena corlissi* Thompson, 1955, and a key for identification of holotrich ciliates of freshwater fishes. J Parasitol 6:217–223. https://doi.org/10.2307/3278995

Imai S, Tsurimaki S, Goto E, Wakita K, Hatai K (2000) *Tetrahymena* infection in Guppy, *Poecilia reticulata*. Fish Pathol 35:67–72. https://doi.org/10.3147/jsfp.35.67

International Commission on Zoological Nomenclature (1999) International code of zoological nomenclature, 4th edn. Tipografia La Garangola, Padova

Jerome CA, Simon EM, Lynn DH (1996) Description of *Tetrahymena empidokyrea* n. sp., a new species in the *Tetrahymena pyriformis* sibling species complex (Ciliophora, Oligohymenophorea), and an assessment of its phylogenetic position using small-subunit rRNA sequences. Can J Zool 74:1898–1906. https://doi.org/10.1139/z96-214

Kazubski SL (1958) Results of investigations carried out on Ciliata and some other parasites of land snails. Wiad Parazytol 4:666

Kazubski SL (1959) Studies on the ciliophoran parasites of the land snails in Poland in the years 1956–1958. J Protozool 6(Suppl):26–39. https://doi.org/10.1111/j.1550-7408.1959.tb04386.x

Kazubski SL (1960) Materialy k poznaniju fauny paraziticheskih infuzorij nazemnych moljuskov Karpat. In: Flora i fauna Karpat (Sbornik rabot). Izvestiya Akademii Nauk SSR, Moskva, pp 220–223

Kazubski SL, Szablewski L (1978) On the morphological variability of *Tetrahymena limacis* (Warren) and *T. rostrata* (Kahl), ciliate parasites of land snails. In: Fourth International Congress on Parasitology, 19–26 August 1978, Section B. Warszawa, p 9.

Kher CP, Doerder FP, Cooper J, Ikonomi P, Achilles-Day U, Küpper FC, Lynn DH (2011) Barcoding *Tetrahymena*: discriminating species and identifying unknowns using the cytochrome *c* oxidase subunit I (cox-1) barcode. Protist 162:2–13. https://doi.org/10.1016/j.protis.2010.03.004

Klein BM (1958) The "dry" silver method and its proper use. J Protozool 5:99–103. https://doi.org/10.1111/j.1550-7408.1958.tb02535.x

Kozloff EN (1946) The morphology and systematic position of a holotrichous ciliate parasitizing *Deroceras agreste* (L.). J Morphol 79:445–465. https://doi.org/10.1002/jmor.1050790305

Kozloff EN (1956a) Experimental infection of the gray garden slug, *Deroceras reticulatum* (Müller), by the holotrichous ciliophoran *Tetrahymena pyriformis* (Ehrenberg). J Protozool 3:17–19. https://doi.org/10.1111/j.1550-7408.1956.tb02425.x

Kozloff EN (1956b) *Tetrahymena limacis* from the terrestrial pulmonate gastropods *Monadenia fidelis* and *Prophysaon andersoni*. J Protozool 3:204–208. https://doi.org/10.1111/j.1550-7408.1956.tb02457.x

Kumar S, Stecher G, Li M, Knyaz C, Tamura K (2018) MEGA X: molecular evolutionary genetics analysis across computing

platforms. Mol Biol Evol 35:1547–1549. https://doi.org/10.1093/molbev/msy096

Lynn DH (2008) The ciliated protozoa. Characterization, classification, and guide to the literature, 3rd edn. Springer, Dordrecht

Lynn DH, Doerder FP (2012) The life and times of *Tetrahymena*. Methods Cell Biol 109:9–27. https://doi.org/10.1016/B978-0-12-385967-9.00002-5

Lynn DH, Strüder-Kypke MC (2006) Species of *Tetrahymena* identical by small subunit rRNA gene sequences are discriminated by mitochondrial cytochrome *c* oxidase I gene sequences. J Eukaryot Microbiol 53:385–387. https://doi.org/10.1111/j.1550-7408.2006.00116.x

Lynn DH, Molloy D, LeBrun R (1981) *Tetrahymena rotunda* n. sp. (Hymenostomatida: Tetrahymenidae), a ciliate parasite of the hemolymph of *Simulium* (Diptera: Simuliidae). Trans Am Microsc Soc 100:134–141. https://doi.org/10.2307/3225796

Lynn DH, Gransden SG, Wright A-DG, Josephson G (2000) Characterization of a new species of the ciliate *Tetrahymena* (Ciliophora: Oligohymenophorea) isolated from the urine of a dog: first report of *Tetrahymena* from a mammal. Acta Protozool 39:289–294

Lynn DH, Doerder FP, Gillis PL, Prosser RS (2018) *Tetrahymena glochidiophila* n. sp., a new species of *Tetrahymena* (Ciliophora) that causes mortality to glochidia larvae of freshwater mussels (Bivalvia). Dis Aquat Org 127:125–136. https://doi.org/10.3354/dao03188

Medlin L, Elwood HJ, Stickel S, Sogin ML (1988) The characterization of enzymatically amplified eukaryotic 16S-like rRNA coding regions. Gene 71:491–499. https://doi.org/10.1016/0378-1119(88)90066-2

Michelson EH (1971) Distribution and pathogenicity of *Tetrahymena limacis* in the slug *Deroceras reticulatum*. Parasitology 62:125–131. https://doi.org/10.1017/S003118200007133X

Miller MA, Pfeiffer W, Schwartz T (2010) Creating the CIPRES Science Gateway for inference of large phylogenetic trees. In: Proceedings of the Gateway Computing Environments Workshop (GCE). Piscataway, NJ, New Orleans, LA, pp 1–8. https://doi.org/10.1109/GCE.2010.5676129

Nguyen LT, Schmidt HA, von Haeseler A, Minh BQ (2015) IQ-TREE: a fast and effective stochastic algorithm for estimating maximum-likelihood phylogenies. Mol Biol Evol 32:268–274. https://doi.org/10.1093/molbev/msu300

Pitsch G, Adamec L, Dirren S, Nitsche F, Šimek K, Sirová D, Posch T (2017) The green *Tetrahymena utricolariae* n. sp. (Ciliophora, Oligohymenophorea) with its endosymbiotic algae (*Micractinium* sp.), living in traps of a carnivorous aquatic plant. J Eukaryot Microbiol 64:322–335. https://doi.org/10.1111/jeu.12369

Prosser RS, Lynn DH, Salerno J, Bennett J, Gillis PL (2018) The facultatively parasitic ciliated protozoan, *Tetrahymena glochidiophila* (Lynn, 2018), causes a reduction in viability of freshwater mussel glochidia. J Invertebr Pathol 57:301–313. https://doi.org/10.1016/j.jip.2018.07.012

Quintela-Alonso P, Nitsche F, Wylezich C, Arndt H, Foissner W (2013) A new *Tetrahymena* (Ciliophora, Oligohymenophorea) from groundwater of Cape Town, South Africa. J Eukaryot Microbiol 60:235–246. https://doi.org/10.1111/jeu.12021

Rambaut A, Drummond AJ, Xie D, Baele G, Suchard MA (2018) Posterior summarization in Bayesian phylogenetics using Tracer 1.7. Syst Biol 67:901–904. https://doi.org/10.1093/sysbio/syy032

Rataj M, Vďačný P (2020) Multi-gene phylogeny of *Tetrahymena* refreshed with three new histophagous species invading freshwater planarians. Parasitol Res 119:1523–1545. https://doi.org/10.1007/s00436-020-06628-0

Reynoldson TB, Bellamy LS (1973) Interspecific competition in lake-dwelling triclads. A laboratory study. Oikos 24:301–313. https://doi.org/10.2307/3543889

Ronquist F, Teslenko M, van der Mark P, Ayres DL, Darling A, Höhna S, Larget B, Liu L, Suchard MA, Huelsenbeck JP (2012) MrBayes 3.2: efficient Bayesian phylogenetic inference and model choice across a large model space. Syst Biol 61:539–542. https://doi.org/10.1093/sysbio/sys029

Schneider CA, Rasband WS, Eliceiri KW (2012) NIH Image to ImageJ: 25 years of image analysis. Nat Methods 9:671–675. https://doi.org/10.1038/nmeth.2089

Segade P, Kher CP, Lynn DH, Iglesias R (2009) Morphological and molecular characterization of renal ciliates infecting farmed snails in Spain. Parasitology 136:771–782. https://doi.org/10.1017/S0031182009006040

Sela I, Ashkenazy H, Katoh K, Pupko T (2015) GUIDANCE2: accurate detection of unreliable alignment regions accounting for the uncertainty of multiple parameters. Nucleic Acids Res 43:W7–W14. https://doi.org/10.1093/nar/gkv318

Simon EM, Nanney DL, Doerder FP (2008) The "*Tetrahymena pyriformis*" complex of cryptic species. Biodivers Conserv 17:365–380. https://doi.org/10.1007/s10531-007-9255-6

Van As JG, Basson L (2004) Ciliophoran (Ciliophora) parasites of terrestrial gastropods. In: Barker GM (ed) Natural Enemies of Terrestrial Molluscs. CABI Publishing, Wallingford, pp 559–578

van Hoek AHAM, Akhmanova AS, Huynen MA, Hackstein JHP (2000) A mitochondrial ancestry of the hydrogenosomes of *Nyctotherus ovalis*. Mol Biol Evol 17:202–206. https://doi.org/10.1093/oxfordjournals.molbev.a026234

Vďačný P, Bourland WA, Orsi W, Epstein SS, Foissner W (2011) Phylogeny and classification of the Litostomatea (Protista, Ciliophora), with emphasis on free-living taxa and the 18S rRNA gene. Mol Phylogenet Evol 59:510–522. https://doi.org/10.1016/j.ympev.2011.02.016

Warren A, Patterson DJ, Dunthorn M, Clamp JC, Achilles-Day UEM, Aescht E, Al-Farraj SA, Al-Quraishy S, Al-Rasheid K, Carr M, Day JG, Dellinger M, El-Serehy HA, FanY GF, Gao S, Gong J, Gupta R, Hu X, Kamra K, Langlois G, Lin X, Lipscomb D, Lobban CS, Luporini P, Lynn DH, Ma H, Macek M, Mackenzie-Dodds J, Makhija S, Mansergh RI, Martín-Cereceda M, McMiller N, Montagnes DJS, Nikolaeva S, Ong'ondo G, Pérez-Uz B, Purushothaman J, Quintela-Alonso P, Rotterová J, Santoferrara L, Shao C, Shen Z, Shi X, Song W, Stoeck T, la Terza A, Vallesi A, Wang M, Weisse T, Wiackowski K, Wu L, Xu K, Yi Z, Zufall R, Agatha S (2017) Beyond the 'Code': a guide to the description and documentation of biodiversity in ciliated protists (Alveolata, Ciliophora). J Eukaryot Microbiol 64:539–544. https://doi.org/10.1111/jeu.12391

Warren E (1932) On a ciliophoran protozoon inhabiting the liver of a slug. Ann Natal Mus 7:1–53

Wilbert N (1975) Eine verbesserte Technik der Protargolimprägnation für Ciliaten. Mikrokosmos 64:171–179

Windsor DA (1959) *Colpoda steinii* and *Tetrahymena limacis* in several terrestrial pulmonate gastropods collected in Illinois. J Protozool 6(Suppl):33–39. https://doi.org/10.1111/j.1550-7408.1959.tb04386.x

Wright JF (1969) The ecology of stream-dwelling triclads. University of Wales, Dissertation

Wright JF (1981) *Tetrahymena pyriformis* (Ehrenberg) and *T. corlissi* Thompson parasitic in stream-dwelling triclads (Platyhelminthes: Turbellaria). J Parasitol 67:131–133. https://doi.org/10.2307/3280799

Yang Z (2015) The BPP program for species tree estimation and species delimitation. Curr Zool 61:854–865. https://doi.org/10.1093/czoolo/61.5.854

Yang Z, Rannala B (2010) Bayesian species delimitation using multilocus sequence data. Proc Natl Acad Sci USA 107:9264–9269. https://doi.org/10.1073/pnas.0913022107

Zahid MT, Shakoori FR, Zulifqar S, Jahan N, Shakoori AR (2014) A new ciliate species, *Tetrahymena farahensis*, isolated from the industrial wastewater and its phylogenetic relationship with other members of the genus *Tetrahymena*. Pakistan J Zool 46:1433–1445

Zhang T, Vďačný P (2020) Re-discovery and novel contributions to morphology and multigene phylogeny of *Myxophyllum steenstrupi* (Ciliophora: Pleuronematida), an obligate symbiont of terrestrial pulmonates. Zool J Linnean Soc. https://doi.org/10.1093/zoolinnean/zlaa095